
Spatiotemporal dynamics of surface sediment characteristics and benthic macrofauna compositions in a temperate high-energy River-dominated Ocean Margin

Lamarque Bastien ^{1,*}, Deflandre Bruno ², Schmidt Sabine ², Bernard Guillaume ¹, Dubosq Nicolas ², Diaz Melanie ², Lavesque Nicolas ¹, Garabetian Frédéric ¹, Grasso Florent ³, Sottolichio Aldo ², Rigaud Sylvain ⁴, Romero-Ramirez Alicia ¹, Cordier Marie-Ange ², Poirier Dominique ², Danilo Martin ², Grémare Antoine ¹

¹ UMR EPOC, Université de Bordeaux, CNRS, UMR 5805, Station Marine d'Arcachon, 2 rue du Professeur Jolyet, 33120, Arcachon, France

² UMR EPOC, Université de Bordeaux, CNRS, UMR 5805, Bâtiments B18/B18N, Allée Geoffroy Saint-Hilaire, CEDEX, 33615, Pessac, France

³ IFREMER, DYNECO/DHYSED, Centre de Bretagne, CS 10070, 29280, Plouzané, France

⁴ Université de Nîmes, EA 7352 CHROME, rue du Dr Georges Salan, 30021, Nîmes, France

* Corresponding author : Bastien Lamarque, email address : bastien.lamarque@u-bordeaux.fr

Abstract :

The benthic compartment of River-dominated Ocean Margins (RiOMar) is largely affected by sedimentary processes, as well as by natural and anthropogenic disturbances. Recent studies have confirmed the major importance of riverine inputs and local hydrodynamics in the spatial structuration of low- and high-energy temperate RiOMar, respectively. Differences in the nature of these structuring factors could also affect the temporal dynamics of these two types of systems. The present study is aiming at: (1) quantifying spatiotemporal changes in surface sediment and benthic macrofauna within the West Gironde Mud Patch (WGMP; high-energy system) over both short (2016–2018) and long (2010–2018) time scales, (2) identifying the main environmental factors controlling those changes, and (3) achieving a comparison with the Rhône River Prodelta (RRP; low-energy system) in view of further characterizing the functioning of the benthic components of these two temperate RiOMar. Surface sediment characteristics (grain size, quantitative and qualitative descriptors of particulate organic matter) and benthic macrofauna compositions were assessed based on 4 seasonal sampling of 5 stations located along a depth gradient within the WGMP. Results highlighted the existence of spatial patterns for both surface sediment and benthic macrofauna, which are cued by local hydrodynamics. Most variables presented seasonal changes. Benthic macrofauna compositions also showed pluri-annual changes, which were attributed to a cicatrization process following a major disturbance caused by the 2014 series of severe winter storms, which underlines the major role of local hydrodynamics in controlling long-term temporal changes in WGMP benthic macrofauna compositions. The comparison with the RRP highlighted major discrepancies between the two systems in the main processes (i.e., hydrodynamics versus river hydrological regime) controlling surface sediment characteristics and benthic macrofauna compositions, which further supports RiOMar typologies derived from meta-analyses mainly achieved on tropical and subtropical systems.

Highlights

► Hydrodynamics leads benthic macrofauna composition in the West Gironde Mud Patch. ► Strong storms could also affect benthic macrofauna temporal dynamics in this area. ► The West Gironde Mud Patch can be characterized as a temperate high-energy system. ► River-dominated Ocean Margins typologies are validated based on macrofauna analysis.

Keywords : RiOMar, West Gironde Mud Patch, North-East Atlantic shelf, Particulate organic matter, Benthic macrofauna, Spatiotemporal changes, Hydrodynamics, Storms

11 **Abbreviations:**
12 AFDW : Ash-Free Dry Weight
13 AJD : Annual Julian Days
14 BSS : Bottom Shear Stress
15 BSS₁₀₀ : Bottom Shear Stress integrated over 100-day periods
16 BSS₃₆₅ : Bottom Shear Stress integrated over 365-day periods
17 Chl-*a* : Chlorophyll-*a*
18 CJD : Cumulated Julian Days
19 D_{0.5} : Median diameter of sediment particles
20 dbRDA : distance-based Redundancy Analysis
21 DISTLM : DISTance-based Linear Model
22 DW : Dry Weight
23 EHAA : Enzymatically Hydrolysable Amino Acids
24 Flow₁₀₀ : River flows integrated over 100-day periods
25 Flow₃₆₅ : River flows integrated over 365-day periods
26 nMDS : non-Metric Multidimensional Scaling
27 PCA : Principal Components Analysis
28 Phaeo-*a* : Phaeophytin-*a*
29 POC : Particulate Organic Carbon
30 POM : Particulate Organic Matter
31 RiOMar : River-dominated Ocean Margin
32 RRP : Rhône River Prodelta
33 SIMPER : SIMilarity PERcentage analysis
34 SIMPROF : SIMilarity PROFile procedure
35 SSA : Sediment Surface Area
36 THAA : Total Hydrolysable Amino Acids
37 WGMP : West Gironde Mud Patch

38

39

40

41

42

43

1 1. INTRODUCTION

2
3 Continental margins are key areas for the marine component of major biogeochemical
4 cycles, accounting for the mineralization of 50 to 80 % of continental Particulate Organic
5 Carbon (POC) inputs (Aller, 1998; Blair and Aller, 2012; Burdige, 2005). Continental
6 margins impacted by major river freshwater and sediment discharges are defined as River-
7 dominated Ocean Margins (RiOMar). RiOMar provide a large variety of ecosystem services
8 including provisioning (e.g. fisheries), regulating (e.g. carbon mineralization/burial) and
9 supporting (e.g. nutrients cycling, habitats) ones (e.g. Aller 1998, Levin et al., 2001, Lansard
10 et al., 2009). Their benthic components constitute the main marine primary depositional areas
11 of riverine particulate inputs (Burdige, 2005; McKee et al., 2004) and it is estimated that
12 RiOMar account for 40 to 50 % of continental POC burial in continental margins (Blair and
13 Aller, 2012; Burdige, 2005; Hedges and Keil, 1995). RiOMar benthic biological
14 compartments (e.g. macrofauna) and biogeochemical fluxes (e.g. mineralization) are largely
15 affected by a variety of natural and anthropogenic disturbances (Aller, 1998; Lansard et al.,
16 2009; Lotze et al., 2006; Rhoads et al., 1985; Tesi et al., 2007; Ulses et al., 2008; Worm et
17 al., 2006).

18 The impact of both sediment discharges and associated organic matter inputs on the
19 structuration of benthic macrofauna communities and biogeochemical functioning of the
20 sediment-water interface has been documented for a large variety of RiOMar (Akoumianaki
21 et al., 2013; Aller and Aller, 1986; Aller and Stupakoff, 1996; Alongi et al., 1992; Bonifácio
22 et al., 2014; Harmelin-Vivien et al., 2009; Rhoads et al., 1985; Wheatcroft, 2006). Mostly
23 based on the analysis of macrofauna vertical distribution within the sediment column and X-
24 ray radiographies, Rhoads et al. (1985) first proposed a conceptual model describing the
25 response of benthic macrofauna and surface sediments to the inputs of major rivers.
26 According to this model, macrofauna spatial distribution is mainly controlled by the
27 interaction between: (1) the physical disturbance induced by intense riverine particles inputs,
28 and (2) Particulate Organic Matter (POM) availability. In proximal (i.e., the closest to the
29 river mouth) parts of RiOMar, high and irregular sedimentation rates induce sedimentary
30 instability, precluding the establishment of mature macrobenthic communities. The high
31 turbidity of river plumes also limits primary production in the water column, resulting in
32 mainly low (refractory) POM concentrations in surface sediments. Accordingly, RiOMar
33 proximal areas are characterized by low bioturbation intensities and low mineralization
34 fluxes. Conversely, in distal (i.e., deeper) parts, moderated sedimentation and enhanced
35 primary production in the water column allow for the establishment of mature macrobenthic
36 communities, high bioturbation intensities and mineralization fluxes.

37 More recent RiOMar typologies have been based on meta-analyses (mostly achieved
38 on tropical and subtropical systems) of geomorphological and biogeochemical processes
39 (Blair and Aller, 2012; McKee et al., 2004). Their results highlighted the major effect of local
40 hydrodynamics on RiOMar morphologies and POC mineralization/burial intensities. This led
41 Blair and Aller (2012) to draw a clear distinction between: (1) low-energy systems, with both
42 high sedimentation rates and carbon preservation (later referred as type 1), and (2) high-
43 energy tidal and/or wave systems with both high sediment oxygenation and low carbon
44 preservation rates (later referred as type 2). Lamarque et al. (2021) recently assessed the main

1 environmental factors responsible for the spatial structuration of temperate type 1 and type 2
2 systems based on the comparison between extensive spatial surveys conducted within the
3 Rhone River Prodelta (RRP; type 1, French Mediterranean coast) and the West Gironde Mud
4 Patch (WGMP; type 2, French Atlantic coast). Their results confirmed the major importance
5 of riverine inputs and local hydrodynamics in the spatial structuration of type 1 and type 2
6 temperate RiOMar, respectively.

7 Such a difference in the nature of their main structuring factors could as well affect
8 the spatiotemporal dynamics of these two types of systems. Seasonal changes in both surface
9 sediment characteristics and benthic macrofauna compositions along a depth gradient have
10 already been addressed within the RRP Bonifácio et al. (2014). Results showed that temporal
11 changes were larger at the most proximal station in relation with changes in river flow. Major
12 changes were observed after a prolonged low-flow period, which allowed for the
13 development of a mature macrobenthic community (otherwise precluded due to high
14 sedimentation rates resulting from POM riverine inputs). Conversely, temporal changes in
15 benthic surface sediment characteristics and benthic macrofauna compositions within the
16 WGMP have only been poorly documented so far. The only available quantitative benthic
17 macrofauna composition data have been collected during a single cruise (during July 2010)
18 and at only 3 stations (Massé et al., 2016). Consequently, the controlling factors and the
19 magnitude of spatiotemporal changes in surface sediment characteristics and benthic
20 macrofauna compositions within the WGMP (taken as an example of temperate type 2
21 RiOMar) are still largely unknown.

22 The present study is aiming at filling this gap by: (1) quantifying spatiotemporal
23 changes in surface sediment characteristics and benthic macrofauna compositions within the
24 WGMP over both short (2016-2018) and long (2010-2018) time scales, (2) identifying the
25 main environmental factors controlling these changes, and (3) achieving a comparison with
26 the RRP in view of further characterizing the functioning of benthic components in temperate
27 type 1 and type 2 RiOMar.

28 29 **2. MATERIALS & METHODS**

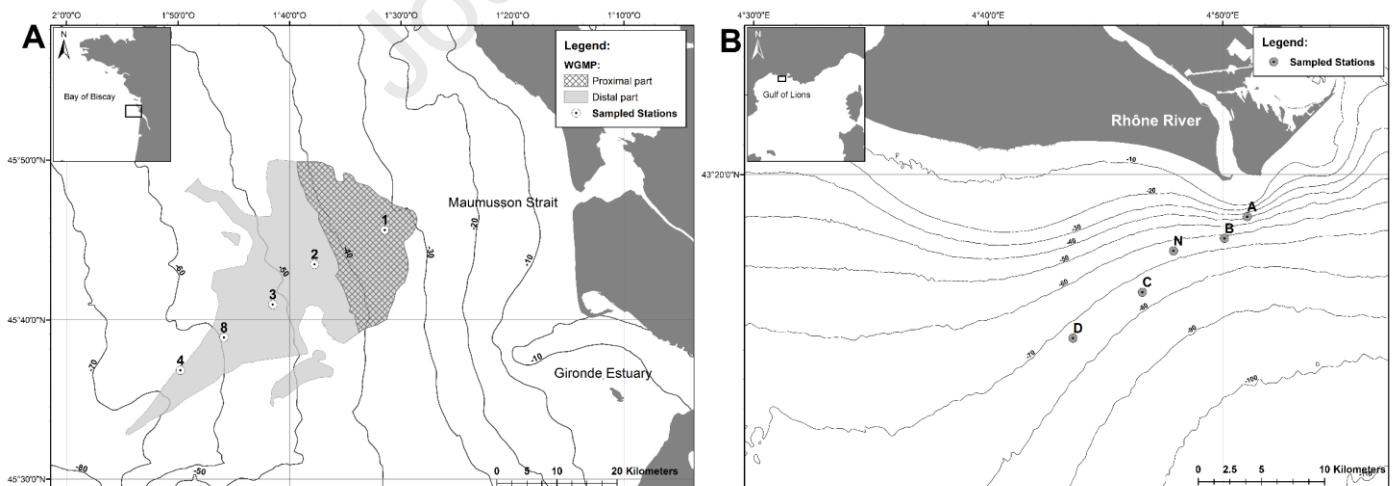
30 31 **2.1 WGMP: Sampling area**

32
33 The WGMP is a 420 km² sedimentary body located in the Bay of Biscay 40 km off
34 the Mouth of the Gironde Estuary, between ca. 30 and 75m depth (Figure 1). This relict
35 paleovalley is the primary depocenter (sedimentation rates between less than 1 and 10 mm.y⁻¹;
36 Dubosq et al. 2021) of fine particles originating from the Gironde Estuary, which has an
37 annual mean water flow of 944 m³.s⁻¹ (Doxaran et al., 2009) with daily flows up to 7,500
38 m³.s⁻¹ during winter floods (Constantin et al., 2018). The WGMP is located in a macro-tidal
39 environment with a tidal range from 1.5 to 5m (Jalón-Rojas et al., 2018). The continental
40 shelf off the Mouth of the Gironde Estuary is periodically submitted to strong swells/waves,
41 which can reach maximal amplitudes of 15 m and periods of 15 s during winter storms (Cirac
42 et al., 2000; Masselink et al., 2016). The sedimentology of the WGMP has been extensively
43 studied based on stratigraphic sequences, palynological data, X-ray radiographies and
44 radiochronographies (Castaing et al., 1979, 1982; Castaing and Allen, 1981; Gadel et al.,

1 1997; Jouanneau et al., 1989; Lesueur et al., 1991, 1996, 2001, 2002; Lesueur and Tastet,
 2 1994; Longère and Dorel, 1970; Parra et al., 1998; Weber et al., 1991). These surveys have
 3 attributed a major role to local hydrodynamics in controlling the spatial structuration of the
 4 WGMP. This paradigm was based on both: (1) the segmentation between a proximal and a
 5 distal part with no modern persistent sedimentation in the former, and (2) the decreasing
 6 frequency of occurrence of vertical erosional sequences within the sediment column with
 7 station depth (Jouanneau et al., 1989; Lesueur et al., 1991, 2001, 2002; Lesueur and Tastet,
 8 1994). It was recently further validated by a synoptic survey of the spatial distributions of
 9 surface sediment characteristics and biological activity traces (Lamarque et al., 2021).

11 2.2. WGMP: Sampling of surface sediment and benthic macrofauna

13 Five stations located along a depth gradient (Figure 1A, Table I) were sampled for
 14 surface sediment characteristics and benthic macrofauna during 4 cruises, which took place
 15 on board of the R/V Côtes de la Manche in October-November 2016 (hereafter October 2016,
 16 JERICObent-1; Deflandre 2016), August 2017 (JERICObent-2; Deflandre 2017), January-
 17 February 2018 (hereafter February 2018; JERICObent-3; Deflandre 2018a) and April-May
 18 2018 (hereafter April 2018; JERICObent-4; (Deflandre, 2018b). Only 4 stations were
 19 sampled in February 2018 due to bad meteorological conditions. During each cruise, 4
 20 sediment cores (10 cm internal diameter) were collected at each station using an Oktopus
 21 GmbH® multiple corer. The upper top 0.5 cm was sliced and immediately frozen (-20°C) on
 22 board. A single core was used to assess sediment grain size, Sediment Surface Area (SSA;
 23 Mayer 1994), POC concentrations (hereafter POC) and $\delta^{13}\text{C}$. The remaining 3 cores were
 24 used to assess chloro-pigment and amino acid concentrations. Benthic macrofauna was
 25 sampled using a 0.25 m² Hamon grab (3 replicates), sieved on a 1 mm mesh and fixed with 4
 26 % formalin.



27 **Figure 1. Sampling:** Map showing the delimitation of: (A) the West Gironde Mud Patch
 28 along the French Atlantic Coast together with the locations of the 5 stations sampled during
 29 the present study. Stations 1, 3 and 4 had also previously been sampled in July 2010 by
 30 Massé et al. (2016); and (B) the Rhône River Prodelta in the Gulf of Lions (NW
 31 Mediterranean) together with the locations of the 5 stations sampled by Bonifácio et al.
 32 (2014) in April 2007, May and December 2008, and July 2011. (See text for details)

2.3. WGMP: Gironde Estuary water flows

Daily water flows of the Gironde Estuary were assessed by summing the flows of its two main tributaries, the Garonne and Dordogne Rivers, measured in Tonneins and Pessac-sur-Dordogne, respectively. Data were provided by the French Ministère de l'Ecologie, du Développement Durable et de l'Energie (<http://www.hydro.eaufrance.fr>).

Table I. *Sampling:* Location (WGS84, degrees, and decimal minutes) and depth of the 5 stations (1, 2, 3, 8, 4) sampled in the West Gironde Mud Patch (WGMP) during the present study and of the 5 stations (A, B, N, C, D) sampled in the Rhône River Prodelta (RRP) by Bonifácio et al. (2014). (See text for details)

System	Station	Latitude (N)	Longitude (W)	Depth (m)
WGMP	1	45°45.580'	1°31.489'	37
	2	45°43.511'	1°37.773'	47.8
	3	45°41.007'	1°41.545'	56.5
	8	45°38.873'	1°45.777'	64.5
	4	45°36.924'	1°49.712'	71.5
RRP	A	43°18.690'	04°51.042'	24
	B	43°18.013'	04°50.068'	54
	N	43°17.626'	04°47.896'	67
	C	43°16.343'	04°46.565'	76
	D	43°14.917'	04°43.613'	74

2.4. WGMP: Local hydrodynamics

At each of the 5 sampled stations (Figure 1, Table I), daily values of Bottom Shear Stress (BSS) were computed from a tridimensional numerical model (Diaz et al., 2020). This model, stretching from the Gironde Estuary to the continental shelf, is based on the MARS3D hydrodynamic model (Lazure and Dumas, 2008) and the WAVE WATCH III[®] wave model (Roland and Ardhuin, 2014). Its curvilinear mesh resolution is ca. 0.5x0.5 km² over the WGMP. The model integrates realistic hydro-meteorological forcing (i.e., wind, tide, surge and river flow). BSS were computed as the combination of their current-induced and wave-induced components following Soulsby's formulation (Soulsby, 1997). A more detailed description can be found in Grasso et al. (2018). Simulations achieved during the present study provided hourly outputs from 2010 to 2018 that were daily compiled and 95th percentiles were used to characterize BSS intensities to account for intense hydrodynamic events. Since BSS correlate negatively with station depths (Lamarque et al., 2021), their temporal changes were presented only for station 3.

2.5. WGMP: Surface sediment characteristics

Grain sizes were measured on aliquots of unreplicated sediment samples using a Malvern[®] Master Sizer laser microgranulometer. Almost all distributions were unimodal and therefore characterized through their median diameter ($D_{0.5}$). SSA was measured on freeze-dried sediment samples, previously degassed overnight at 150°C, using a Gemini[®] VII Surface Area Analyzer (Micromeritics[®] 2390a model) with the multi-point Brunauer-Emmett-Teller method (Mayer, 1994). POC were assayed using a LECO[®] CS 200 analyzer, after 2M HCl overnight decarbonation (Etcheber et al., 1999) of previously freeze-dried unreplicated sediment samples. They were normalized for SSA (i.e., expressed in terms of mass per SSA) since these two parameters were assessed on the same sediment core at each combination of stations*dates.

Total and Enzymatically Hydrolysable Amino Acids (THAA and EHAA) were analyzed on triplicates for each of the 3 sampled cores. THAA were extracted through acid hydrolysis (6M HCl, 100°C, 24h). EHAA were extracted following the biomimetic approach proposed by Mayer et al. (1995). THAA and EHAA were derivatized to form fluorescent amino compounds, which were separated by reverse phase High-Performance Liquid Chromatography (Agilent[®] 1260 INFINITY) on a Phenomenex[®] Kinetex 5 μ m EVO C18 column and detected using a 338 nm excitation wavelength. Their concentrations (hereafter THAA and EHAA) were expressed in terms of mass per mass of sediment Dry Weight (DW) since SSA were not measured on the same sediment cores.

Chlorophyll-*a* and Phaeophytin-*a* were assayed on unreplicated thawed frozen (-20°C) sediment samples after overnight acetone extraction (90 % final concentration) using a Perkin Elmer[®] LS-55 spectrofluorometer following Neveux & Lantoiné (1993). Their concentrations (hereafter Chl-*a* and Phaeo-*a*) were expressed in terms of mass per mass of sediment DW since SSA were not measured on the same sediment cores.

Chl-*a*/(Chl-*a* + Phaeo-*a*) ratios (hereafter Chl-*a*/(Chl-*a* + Phaeo-*a*)) were used as a lability index of vegetal biomass (Bonifácio et al., 2014; Pastor et al., 2011) and EHAA/THAA ratios (hereafter EHAA/THAA) were used as a lability index of bulk sedimentary organics (Bonifácio et al., 2014; Grémare et al., 2005; Medernach et al., 2001; Pastor et al., 2011; Wakeham et al., 1997).

For the analysis of POC isotopic ratio, duplicated freeze-dried sediment samples were decarbonated (1M HCl) and later analyzed using a Thermo Scientific[®] Delta V plus IRMS coupled with a Thermo Scientific[®] Flash 2000 EA. Raw measurements were converted in usual $\delta^{13}\text{C}$ units (Coplen, 2011).

2.6. WGMP: benthic macrofauna

Macrofauna was sorted, identified to the lowest tractable taxonomic level and counted. Species richness was computed on pooled replicates for each combination of stations and dates. Biomasses (Ash-Free Dry Weights, AFDW) were measured for each individual taxon as ignition loss (450°C, 4 h) except for Ophiuridae for which an allometric regression was used to account for arm loss: $\text{AFDW} = 0.0111 \times (\text{disk diameter})^{2.5268}$ (where

1 AFDW and disk diameter are expressed in g and mm, respectively; N. Lavesque, personal
2 communication). Abundances and biomasses were standardized per m².

4 **2.7. WGMP: data analysis**

6 To identify the most pertinent time scales for assessing the structuring role of river
7 flow and local hydrodynamics on spatiotemporal changes in surface sediment characteristics
8 (i.e., mean: SSA, POC/SSA, Chl-*a*, Phaeo-*a*, Chl-*a*/(Chl-*a*+Phaeo-*a*), THAA, EHAA,
9 EHAA/THAA and $\delta^{13}\text{C}$) and benthic macrofauna compositions, the Pearson correlation
10 coefficients linking their similarity matrices (Euclidean and Bray-Curtis distances,
11 respectively) with similarity matrices based on either integrated river flows or integrated BSS
12 were computed. This was achieved using R version 3.6.1 (R Core Team, 2019) with the
13 additional packages *vegan* (Oksanen et al., 2019), *BBmisc* (Bischi et al., 2017) and *Hmisc*
14 (Harrell, 2021) for river flows and BSS integrated over 1 to 365 days before each of the 4
15 cruises.

16 For the same surface sediment characteristics (same variables as described above),
17 hierarchical clustering (Euclidean distance and average group linking) and Principal
18 Components Analysis (PCA) were used to define groups of stations**sampling dates* and to
19 assess relationships between variables. A SIMilarity PROFile procedure (SIMPROF, Clarke
20 et al. 2008) was used to test for the statistical significance of between-group differences.
21 SIMilarity PERcentage analysis (SIMPER, Clarke 1993) was used to identify the sediment
22 characteristics contributing most to those differences. A DISTance-based Linear Model
23 (DISTLM) was established to assess the potential contributions of river flows and BSS to
24 spatiotemporal changes in surface sediment characteristics. This model was built using the
25 Best selection procedure (Anderson et al., 2008) and the AIC selection criterion (Akaike,
26 1973). It was represented in a multidimensional space through a distance-based Redundancy
27 Analysis (dbRDA; Anderson et al. 2008). All surface sediment analyses were performed on
28 normalized data and river flows and BSS were integrated over both 100- (i.e., seasonal) and
29 365- (i.e., annual) day periods based on results of the above-described correlation analysis.
30 Station depth, Annual Julian Days (i.e., AJD: the number of days since the beginning of the
31 sampling year), and Cumulated Julian Days (i.e., CJD: the number of days since the first day
32 of the October 2016 cruise) were introduced as supplementary variables. The same approach
33 was used for benthic macrofauna abundances. However, in this case and because of the use of
34 the Bray-Curtis similarity, a non-Metric Multidimensional Scaling (nMDS) was achieved
35 instead of a PCA. Moreover, an intermediate DISTLM/dbRDA was achieved using
36 macrofauna composition as response variable and normalized surface sediment
37 characteristics as predictor variables. POC, Phaeo-*a* and EHAA were excluded from this last
38 procedure due to their strong correlation with other surface sediment characteristics.

39 A long-term comparison with macrofauna abundance data collected in July 2010 at
40 stations 1, 3 and 4 (i.e., station E, C and W in Massé et al. 2016) was achieved through
41 hierarchical clustering (Bray-Curtis distance and average group linking) and nMDS together
42 with the SIMPROF and SIMPER procedures. To avoid possible inconsistencies in taxa

1 identification, these analyses were conducted at the genus level (square-root transformed
2 data).

3 All multivariate analyses were computed using the PRIMER[®] 6 software package
4 (Clarke and Warwick, 2001) with the PERMANOVA+ add-on (Anderson et al., 2008).

7 **2.8. Comparison between the WGMP and the RRP**

9 Intra-station temporal variabilities in sediment surface characteristics and benthic
10 macrofauna compositions were compared in the WGMP (4 cruises between 2016 and 2018 as
11 described above) and the RRP. The latter was sampled by Bonifácio et al. (2014) during 4
12 cruises carried out in April 2007, May and December 2008, and July 2011 (corresponding to
13 different hydrological regimes of the Rhône River) at 5 stations located along a gradient of
14 distance from the mouth of the Rhone River taking into account the preferential direction of
15 its plume (Figure 1B; Table I).

16 These comparisons were based on the information contained in dissimilarity matrices
17 computed using: (1) $D_{0.5}$, POC, Chl-*a*, Phaeo-*a*, Chl-*a*/(Chl-*a*+Phaeo-*a*), THAA, EHAA and
18 EHAA/THAA (i.e., all the surface sediment characteristics measured during both studies),
19 and (2) benthic macrofauna abundances. The sums of squared distances from individual
20 points (i.e., station*sampling date) to their group (i.e., station) centroids were computed for
21 each station (following Anderson 2001 and Anderson et al. 2008) and used as an indices of
22 intra-station temporal variability after standardization for the number of sampling dates.
23 Variables contributing most to intra-station temporal variabilities were also identified.

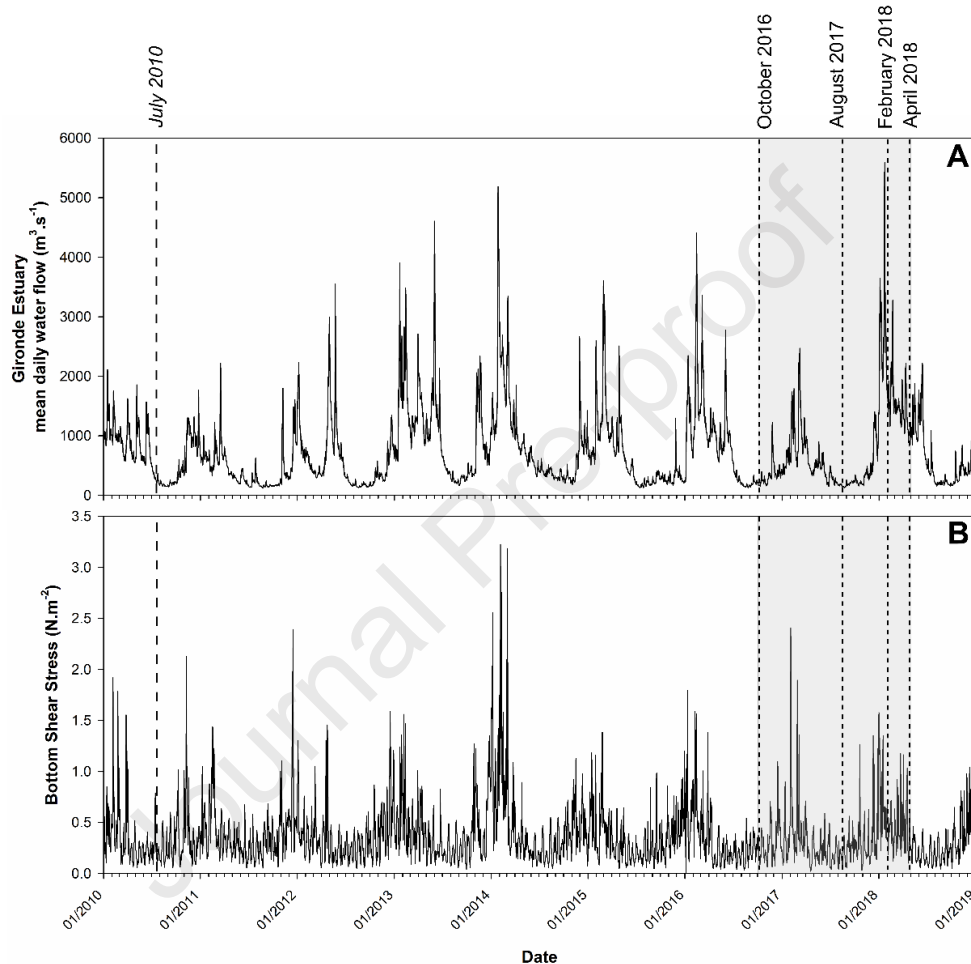
25 **3. RESULTS**

27 **3.1. WGMP: Water flows and Bottom Shear Stress over the 2010-2018 period**

28 Water flows presented a clear seasonal pattern with winter floods (peaks up to 5 590
29 $m^3 \cdot s^{-1}$ on January 23 2018) and low-flow periods during summer and fall (Figure 2A). Over
30 the whole 2010-2018 period, major events were the January 2018 and to a slightly lower
31 extent the January 2014 floods. Between October 2016 and April 2018, there were clear inter-
32 annual differences in water flows during the high-flow period as indicated by the moderate
33 values recorded during the 2016-2017 as opposed to 2017-2018 winter. The July 2010 cruise
34 (Massé et al., 2016) was achieved immediately after the end of a high-flow period. The
35 October 2016 and August 2017 cruises were achieved during low-flow periods (112 and 67
36 days after the end of the preceding high-flow period, respectively). Conversely, both the
37 February 2018 and April 2018 cruises took place during a high-flow period, respectively 5
38 and 87 days after the January 2018 flood.

39 BSS also showed a clear seasonal pattern with a succession of peaks induced by
40 winter storms and conversely low values during summer and fall (Figure 2B). Over the whole
41 2010-2018 period, the major event was the succession of peaks (i.e., up to 3.23 $N \cdot m^{-2}$)
42 induced by the repetition of strong storms during the 2013-2014 winter. The July 2010 cruise
43 (Massé et al. 2016) was achieved at the end of a low-BSS period. During the 2016-2018
44

1 period, there were slight differences between temporal changes in water flows and BSS since:
 2 (1) high-BSS periods generally preceded high-flow periods, and (2) highest BSS (up to 2.40
 3 $\text{N}\cdot\text{m}^{-2}$ on February 3 2017) were recorded during 2016-2017 *versus* 2018 for highest water
 4 flows. Nevertheless, both the October 2016 and August 2017 cruises were conducted during
 5 low-BSS periods (i.e., $<0.5 \text{ N}\cdot\text{m}^{-2}$) as opposed to the February 2018 and April 2018 cruises,
 6 which both took place during the 2017-2018 high-BSS period.



7

8 **Figure 2.** WGMP: Temporal changes in Gironde Estuary mean daily water flows (A) and in
 9 the 95th percentile of Bottom Shear Stress at station 3 (B) between 2010-2018. Short-dashed
 10 lines indicate the 4 cruises achieved in 2016-2018 (grey area) and the long-dashed line
 11 indicates the July 2010 cruise (Massé et al., 2016).

12

13 3.2. WGMP: Short-term (2016-2018) spatiotemporal changes in surface sediment 14 characteristics

15

16 $D_{0.5}$ of surface sediments were usually larger (60, 76 and 92 μm in October 2016,
 17 August 2017 and February 2018, respectively) and much more variable (16 μm in April
 18 2018) at station 1 (Table II, Figure 3A). At all other stations, $D_{0.5}$ were homogeneous (mean
 19 values around 20 μm) and temporally stable. Spatiotemporal changes in $\delta^{13}\text{C}$ were limited

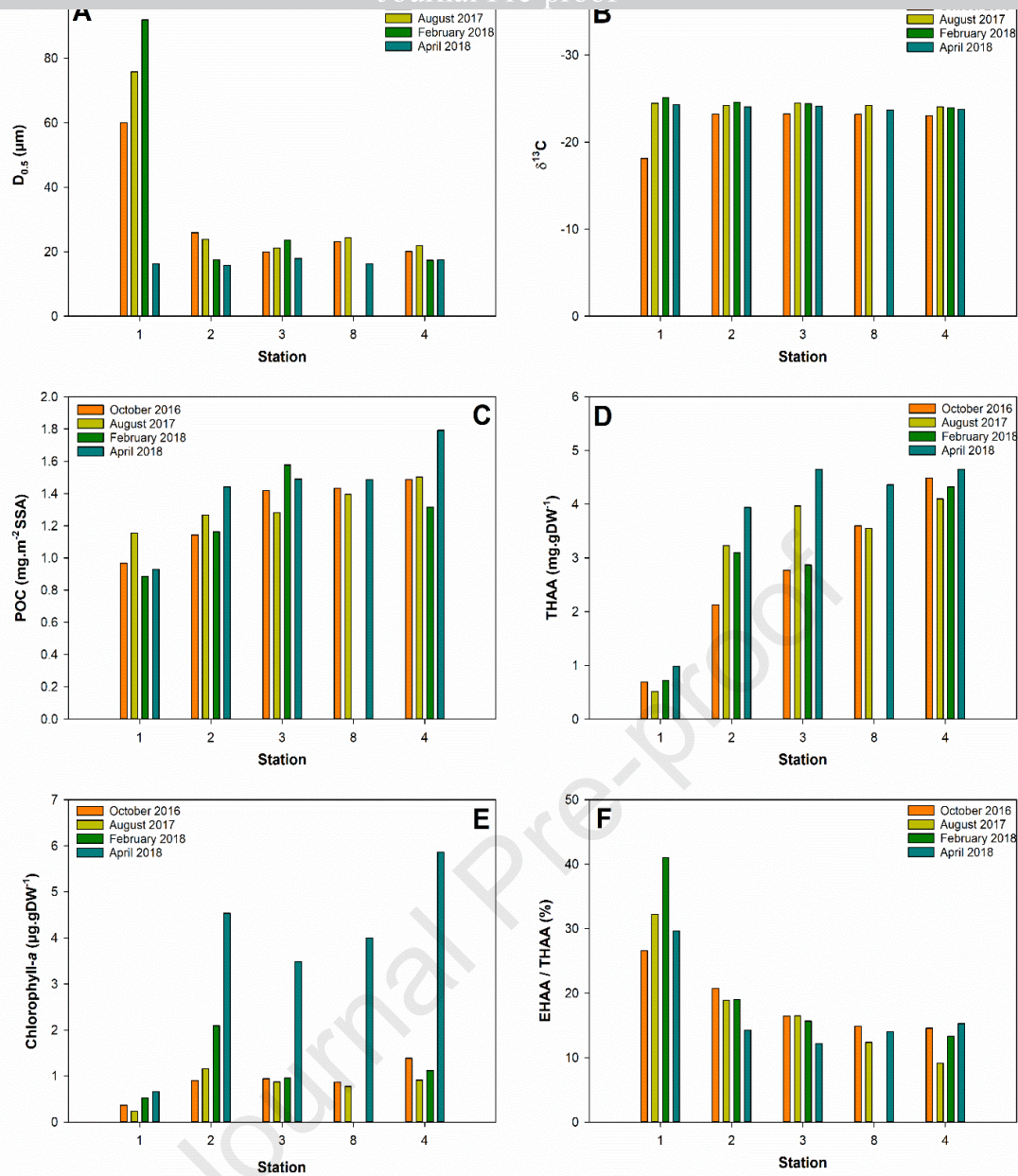
1 (i.e., between -25.12 and -23.01 ‰) with the exception of station 1 in October 2016 (-18.11
2 ‰, Table II, Figure 3B). POC clearly increased with station depth (i.e., from stations 1 to 4),
3 with a maximal value of 1.79 mg.m^{-2} SSA at station 4 during April 2018 (Table II, Figure
4 3C). The only exception to this pattern was February 2018 with a maximal value of 1.58
5 mg.m^{-2} SSA at station 3. At station 4, POC was higher in April 2018 than during the 3 other
6 cruises (mean value of 1.44 mg.m^{-2} SSA). THAA also increased with station depth (Table II,
7 Figure 3D). THAA ranged from 0.51 mg.gDW^{-1} (station 1 in August 2017) to 4.65 mg.gDW^{-1}
8 ¹ (stations 3 and 4 in April 2018). Temporal changes in THAA were lower at station 4
9 (variation coefficient of 5.4 % *versus* a mean of 22.0 % at the 4 other stations). Chl-*a* at
10 station 1 were low (i.e., between 0.23 and $0.66 \text{ }\mu\text{g.gDW}^{-1}$ in August 2017 and April 2018,
11 respectively) during all cruises, (Table II, Figure 3E). At all other stations, Chl-*a* were much
12 higher in April 2018 (with a maximal value of $5.86 \text{ }\mu\text{g.gDW}^{-1}$ at station 4) than during the 3
13 other cruises (mean value of $1.09 \pm 0.37 \text{ }\mu\text{g.gDW}^{-1}$ for stations 2, 3, 8 and 4). EHAA/THAA
14 clearly decreased with station depth (Table II, Figure 3F). EHAA/THAA was maximal (41.0
15 %) at station 1 in February 2018 and minimal (9.1 %) at station 4 in August 2017. Temporal
16 changes were larger at stations 4 and 1 (variation coefficient of 21.0 and 19.2 %, respectively)
17 than at the 3 other stations (mean variation coefficient of 12.7 %).

18

19

20

21

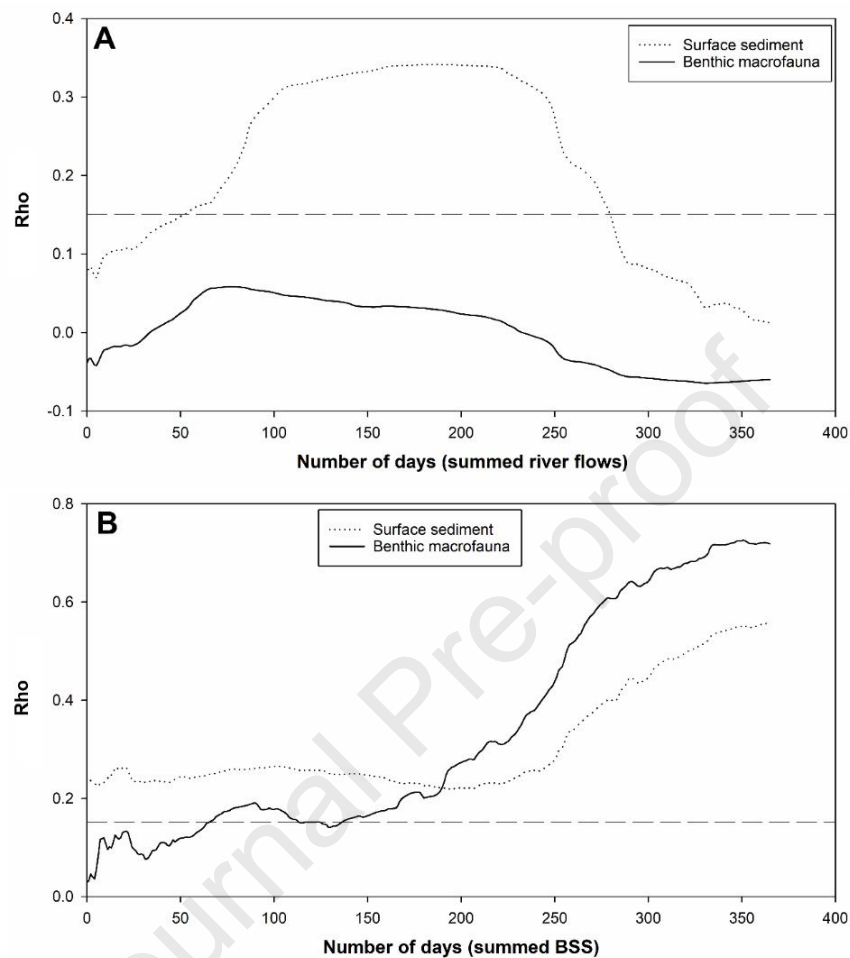


1 **Figure 3.** *WGMP*: Spatiotemporal changes in the (mean) values of surface sediment
 2 characteristics during the 4 cruises achieved between 2016 and 2018: Median grain sizes
 3 ($D_{0.5}$; **A**), $\delta^{13}\text{C}$ (**B**), Particulate Organic Carbon concentrations normalized by SSA (POC; **C**),
 4 Total Hydrolysable Amino Acids concentration (THAA; **D**), Chlorophyll-*a* concentrations
 5 (**E**), and Enzymatically/Total Hydrolysable Amino Acids ratios (EHAA/THAA; **F**). Stations
 6 are ordered according to their depth.

7

8 The Pearson correlation coefficients linking the similarity matrix based on integrated
 9 river flows and those based on either surface sediment characteristics or benthic macrofauna
 10 compositions are shown in Figure 4A. When using surface sediment characteristics,
 11 correlation coefficients first increased with integration period durations, became significant
 12 for a 53-day integration period and reached a maximal value of 0.34 for integration periods
 13 between 156 and 222 days. They then decreased constantly down to a value of 0.01 for an

1 integration period of 365 days. When using benthic macrofauna compositions, correlation
 2 coefficients remained insignificant over the whole range of river flow integration periods.

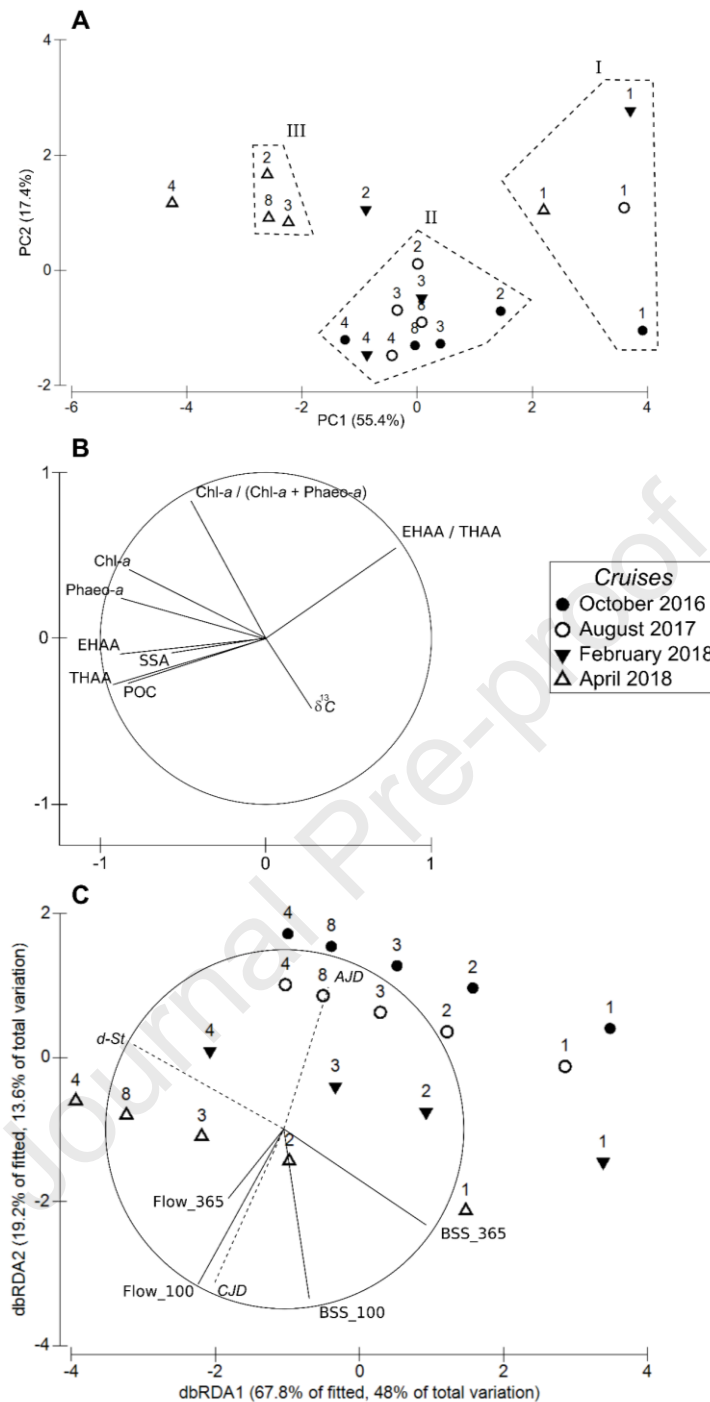


3 **Figure 4. WGMP:** Changes in the Pearson correlation coefficient (Rho) linking the similarity
 4 matrices based on either surface sediment characteristics or benthic macrofauna
 5 compositions (data collected between 2016 and 2018) with river flows (A) and BSS (B)
 6 integrated over 1 to 365-day time periods preceding the 4 cruises. Dotted lines represent 5 %
 7 significance thresholds.

8
 9 The Pearson correlation coefficients linking the similarity matrix based on integrated
 10 BSS and those based on either surface sediment characteristics or benthic macrofauna
 11 compositions are shown in Figure 4B. In both cases, they increased with BSS integration
 12 periods and their maximal values were reached around 1-year (i.e., 0.56 and 0.73 at 365 and
 13 351 days for surface sediment characteristics and benthic macrofauna compositions,
 14 respectively). However, the patterns of changes with increasing integration periods clearly
 15 differed. When using surface sediment characteristics, correlation coefficients were always
 16 significant and almost constant for integration periods between 1 to ca. 250 days. Conversely,
 17 when using benthic macrofauna compositions, correlation coefficients were not significant
 18 for integration periods shorter than 65 days. They then presented a relative maximum (0.19
 19 for a 90-day integration period) before almost constantly increasing for integration periods
 20 longer than 130 days.

1
2 The first two components of the PCA based on surface sediment characteristics
3 accounted for 72.8 % (i.e., 55.4 % and 17.4 %, respectively) of their total variance (Figure
4 5A). Hierarchical clustering and the associated SIMPROF procedure resulted in the
5 identification of 3 groups and 2 “isolated” stations*dates (Figure 5A). “Isolated”
6 stations*dates consisted of station 2 in February 2018 and station 4 in April 2018. Group I
7 was exclusively composed of stations 1 (all sampling dates). Group II was composed of all
8 remaining stations*dates except for the April 2018 cruise. All the stations sampled during this
9 cruise clustered into group III, except stations 1 (Group I) and 4 (isolated). The first principal
10 component was mostly defined by the opposition between the quantitative and qualitative
11 characteristics of surface sedimentary organics with THAA, EHAA, POC, Chl-*a*, Phaeo-*a*
12 and POC concentrations on one side and EHAA/THAA on the other. The second component
13 was mostly defined by the Chl-*a*/(Chl-*a*+Phaeo-*a*) and to a lesser extent EHAA/THAA
14 (Figure 5B). The average dissimilarity between groups I and II was 25.0 %, with
15 EHAA/THAA contributing for 20 %, $\delta^{13}\text{C}$ for 16.9 %, THAA for 16.3 %, and EHAA for
16 14.9 %. The average dissimilarity between groups II and III was 13.5 %, with Chl-*a*/(Chl-
17 *a*+Phaeo-*a*) (37.3 %), Chl-*a* (27.1 %) and Phaeo-*a* (16.5 %) contributing most. Station
18 2*February 2018 differed from group II (average dissimilarity of 10.8 %) due to higher SSA
19 (contributing for 33.9 %), Chl-*a*/(Chl-*a*+Phaeo-*a*) (contributing for 33.7 %) and lower POC
20 (contributing for 10.7 %). Station 4*April 2018 differed from group III (average dissimilarity
21 of 8.2 %) due to higher Phaeo-*a* (contributing for 38.0 %), POC (contributing for 22.5 %) and
22 Chl-*a* (contributing for 17.5 %).

23 The DISTLM included river flows and BSS integrated over both 100- and 365-day
24 periods (hereafter Flow₁₀₀, Flow₃₆₅, BSS₁₀₀ and BSS₃₆₅) as independent variables. It explained
25 70.7 % of the total variance of surface sediment characteristics. Its representation through the
26 first plane of the dbRDA accounted for 61.6 % of this total variance and showed two main
27 orientations (Figure 5C). The first one, mainly along the first component of the dbRDA,
28 corresponded to the positioning of the stations along the depth gradient and was mainly cued
29 by BSS₃₆₅. The second one, mainly along the second component of the dbRDA, separated the
30 4 cruises and was mainly cued by Flow₁₀₀ and to a lesser extent BSS₁₀₀. CJD and AJD
31 correlated significantly ($p < 0.05$) with this second orientation. This correlation was slightly
32 higher for CJD ($r = 0.934$ versus $r = 0.822$).



1 **Figure 5.** WGMP: Multivariate analyses of surface sediment characteristics recorded
 2 between 2016 and 2018. Projection of stations*cruises on the first plane of a Principal
 3 Component Analysis (A). Figures refer to stations and symbols to cruises. Dotted lines
 4 indicate groups of stations*cruises issued from hierarchical clustering. Correlations of the
 5 variables with the first two principal components (B). Distance-based Redundancy Analysis
 6 based on integrated BSS and river flows (C). Station depth (*d-St*), Annual Julian Days (*AJD*)
 7 and Cumulated Julian Days (*CJD*) were used as supplementary variables. SSA: Sediment
 8 Surface Area; POC: Particulate Organic Carbon; Chl-*a*: Chlorophyll-*a*; Phaeo-*a*:
 9 Phaeophytin-*a*; THAA; Total Hydrolysable Amino Acids; EHAA: Enzymatically
 10 Hydrolysable Amino Acids; BSS_100 and BSS_365: integrated Bottom Shear Stress over
 11 100 and 365 days; Flow_100 and Flow_365: integrated river flows over 100 and 365 days.
 12 (See text for details)

1 3.3. WGMP: Short-term (2016-2018) spatiotemporal changes in benthic macrofauna 2 compositions

3

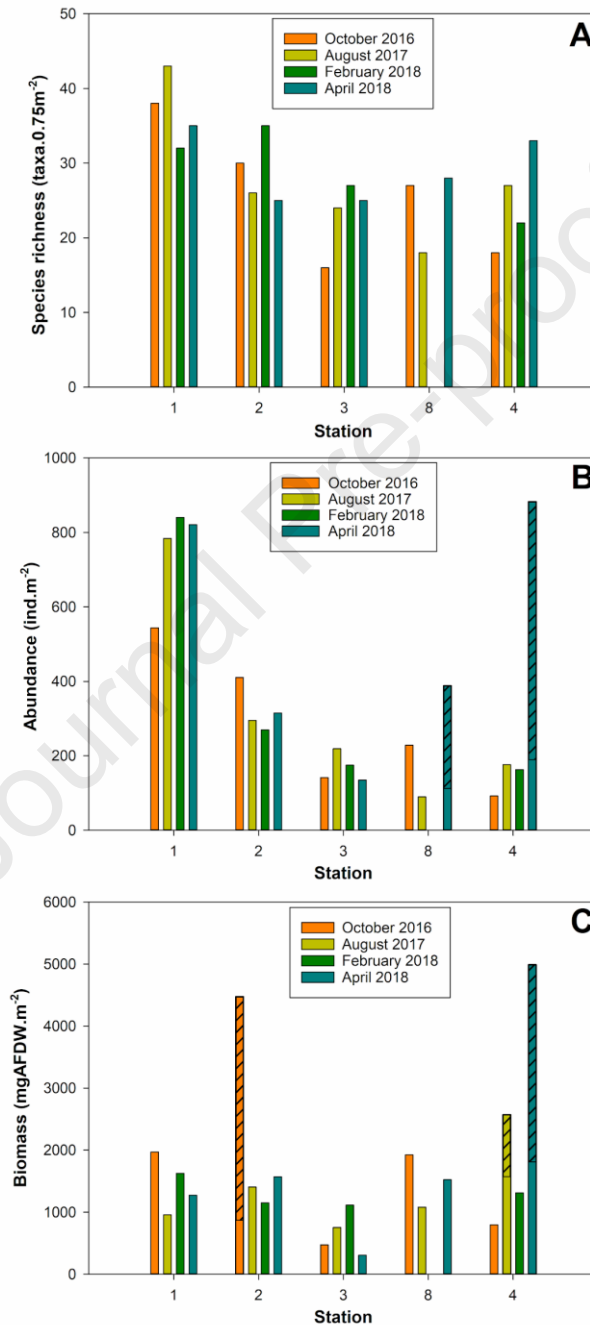
4

5

6

7

Overall, 6391 specimens belonging to 146 taxa were collected and identified (123 taxa after pooling species at the *Ampelisca*, *Glycera* and *Nephtys* genus) during the 4 cruises. Molluscs (mainly abundant at stations 1 and 2) represented 34 % of total macrofauna abundance, followed by polychaetes (27.8 %), echinoderms (22 %) and crustaceans (13.4 %).



8 **Figure 6.** WGMP: Spatiotemporal changes in the (mean) values of main univariate benthic
9 macrofauna characteristics recorded between 2016 and 2018: species richness (A), abundance
10 (B), and biomass (C). Hatching corresponds to the exceptional presence of: (1) numerous
11 individuals of a single taxon for abundance barplot and (2), high biomass of a single taxon for
12 biomass barplot. Stations are ordered according to their depth.

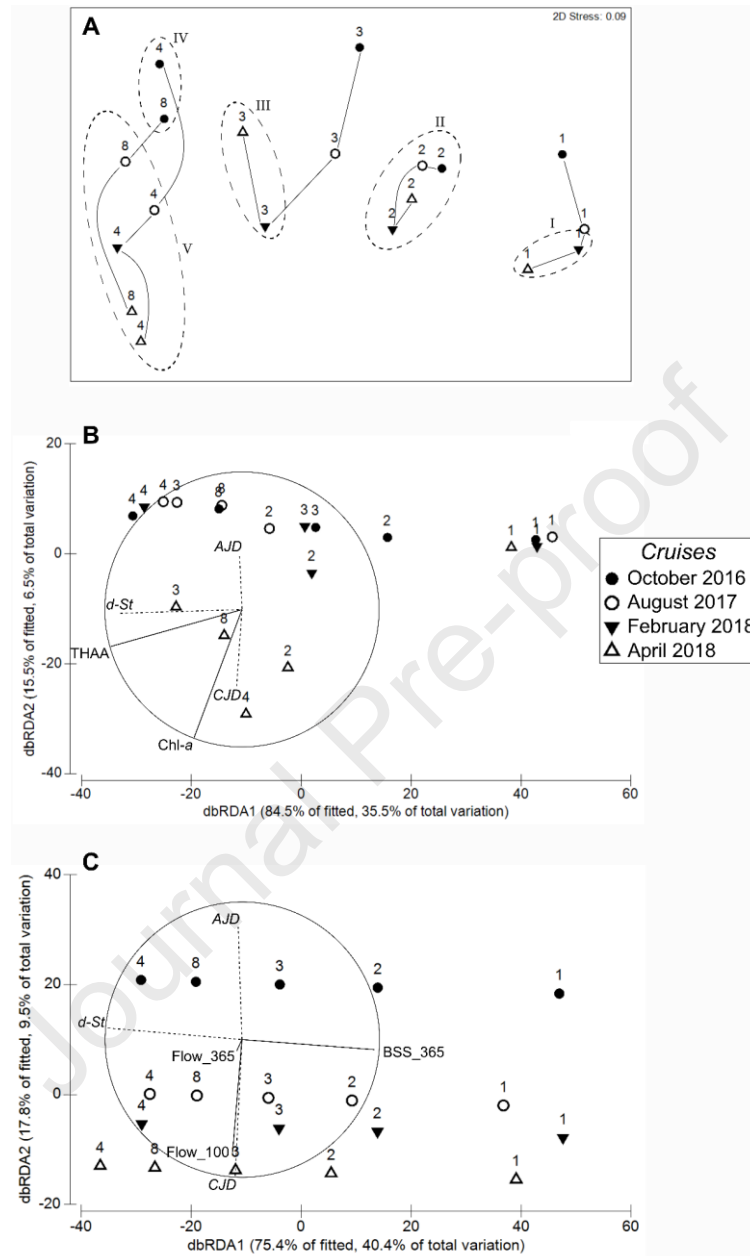
1 Species richness did not show any clear spatiotemporal pattern (Table II, Figure 6A).
 2 It seemed higher at station 1, with a maximum of 43 taxa in August 2017. It tended to
 3 decrease from stations 1 to 3, where a minimal value of 16 taxa was recorded in October
 4 2016. Species richness then seemed to increase from stations 3 to 4 in August 2017 and April
 5 2018. Equitability tended to be lower at stations 1 and 2 than at stations 3, 8 and 4 (Table II).
 6 It was temporally more stable at stations 1 and 2 than at stations 8 and 4, whose variability
 7 resulted from low values in April 2018 caused by the exceptionally high abundances of two
 8 species (see below). Mean macrobenthic abundances were between 882.7 (station 4*April
 9 2018) and 89.3 (station 8*August 2017) individuals per m² (Table II, Figure 6B).
 10 Abundances were higher at station 1 and tended to decrease with station depth. Only stations
 11 8*April 2018 and 4*April 2018 differed from this general pattern with especially high values
 12 due to high densities of *Ampelisca spp.* (182.7 and 593.3 individuals per m² at station 8 and 4
 13 respectively) and *Hyala vitrea* (93.3 and 100.0 individuals per m² at stations 8 and 4
 14 respectively). Changes in mean macrobenthic biomasses did not show any clear
 15 spatiotemporal pattern (Table II, Figure 6C) and were characterized by the occurrence of 3
 16 outliers featuring high values. The high biomass recorded for station 2*October 2016 resulted
 17 from the presence of both a single individual of *Asterias rubens* (2019.0 mgAFDW) and a
 18 high biomass of numerous individuals (i.e., 57.3 per m²) of *Abra alba* (910.6 mgAFDW.m⁻²).
 19 The high biomasses recorded for station 4*August 2017 and station 4*April 2018 both
 20 resulted from the presence of single individuals of *Cereus pedunculatus* in August 2017
 21 (747.0 mgAFDW) and of *Nephrops norvegicus* in April 2018 (2379.2 mgAFDW).

22
 23 The nMDS based on macrofauna abundance data collected between 2016 and 2018 is
 24 shown in Figure 7A. The horizontal dimension of the reduced space corresponded the order
 25 of stations along the depth gradient, reflecting the progressive change in benthic macrofauna
 26 compositions with station depth. For all stations, the vertical dimension of the reduced space
 27 mostly separated sampling cruises. The dispersion of the different cruises for each station
 28 suggests that between-cruises changes in benthic macrofauna compositions were larger at
 29 deep (i.e., stations 3, 4 and 8) than at shallow (i.e., stations 1 and 2) stations. The hierarchical
 30 clustering further confirmed this pattern with the identification of 5 groups: (I) station 1 in
 31 February and April 2018, (II) station 2 during all cruises, (III) station 3 in February and April
 32 2018, (IV) stations 8 and 4 in October 2016, and (V) stations 8 and 4 in August 2017,
 33 February 2018 and April 2018. Between-groups, between isolated stations*dates, and isolated
 34 stations *versus* groups dissimilarities resulted from low contributions of numerous taxa.
 35 Contributions to spatial changes were determined through the assessments of species
 36 contributions to between-clusters dissimilarities. Average dissimilarity between groups I and
 37 II (i.e., between stations 1 and 2) was 48.9 % with *Kurtiella bidentata* (16.3 %), *Nucula*
 38 *nitidosa* (6.0 %), *Cylichna cylindracea* (4.4 %) and *Venus casina* (4.1 %) contributing most,
 39 and being more abundant in stations of group I. Average dissimilarity between groups II and
 40 III (i.e., between stations 2 and 3) was 54.2 % with *Amphiura filiformis* (8.7 %), *K. bidentata*
 41 (6.3 %), *A. alba* (5.7 %) and *Ophiura ophiura* (5.6 %) contributing most, and being more
 42 abundant in stations of group II. Average dissimilarity between groups III and IV (i.e.,
 43 between stations 3 and 8 and 4) was 54.6 % with *A. filiformis* (10.5 %, more abundant in
 44 group III), *Spiophanes afer* (5.8 %, more abundant in group IV), *Ancistrosyllis groenlandica*

1 (5.7 %, more abundant in group III) and *Ampharete lindstroemi* (5.1 %, more abundant in
 2 group IV) contributing most. Average dissimilarity between groups III and V was 53.0 %
 3 with *Ampelisca spp.* (9.8 %, more abundant in group V), *A. filiformis* (9.7 %, more abundant
 4 in group III), *Mediomastus sp.* (4.4 %, more abundant in group V) and *Hyala vitrea* (4.1 %, more
 5 abundant in group V) contributing most. Contributions to temporal changes were
 6 determined through the assessments of species contributions to dissimilarities between (1)
 7 isolated stations*dates corresponding to the same station, (2) isolated stations*dates and
 8 groups containing the same station, and (3) dissimilarities between groups containing the
 9 same stations (i.e., groups IV and V). Here again, dissimilarities were due to low
 10 contributions of numerous taxa. Average dissimilarity between station 1*October 2016 and
 11 others stations 1*sampling dates was 42.0 % with *K. bidentata* (8.4 %, less abundant in
 12 October 2016), *A. alba* (7.5 %, more abundant in October 2016), *A. filiformis* (6.9 %, less
 13 abundant in October 2016), and *V. Casina* (3.8 %, absent in October 2016) contributing most.
 14 Average dissimilarity between station 3*October 2016 and station 3*August 2017 was 48.2
 15 %, with *A. filiformis* (13.4 %), *A. lindstroemi* (8.4 %), *Varicorbula gibba* (7.5 %) and *S. afer*
 16 (6.2 %) contributing most. With the exception of *A. filiformis*, all these taxa were more
 17 abundant in October 2016. Average dissimilarity between station 3*August 2017 and group
 18 III (the other sampling dates of stations 3) was 43.7 %, with *A. filiformis* (11.3 %, more
 19 abundant in August 2017), *Ampelisca spp.* (8.1 %, absent in August 2017), *K. bidentata* (7.2
 20 %, more abundant in August 2017) and *A. groenlandica* (6.9 %, absent in August 2017)
 21 contributing most. Average dissimilarity between groups IV (stations 8 and 4 sampled in
 22 October 2016) and V (other stations 8 and 4 sampling dates) was 51.8 % with *Ampelisca spp.*
 23 (12.5 %), *Mediomastus sp.* (7.0 %), *H. vitrea* (4.8 %) and *S. afer* (4.7 %) contributing most.
 24 With the exception of *S. afer*, these taxa were more abundant at stations of group V.

25
 26 The DISTLM involving surface sediment characteristics as predatory variables
 27 included THAA and Chl-*a*. It explained 42.0 % of the total variance of benthic macrofauna
 28 compositions. Its representation through the first plane of the dbRDA also accounted for 42.0
 29 % of this total variance and showed two main orientations (Figure 7B). The first one, mainly
 30 along the first component of the dbRDA, corresponded to the positioning of the stations
 31 along the depth gradient and was mainly cued by THAA. The second one, mainly along the
 32 second component of the dbRDA, separated stations (except station 1) sampled during April
 33 2018 from all other stations*dates, and was mainly cued by Chl-*a* concentrations. CJD
 34 correlated significantly with this second orientation ($r = 0.560$, $p < 0.05$) but not AJD ($r =$
 35 0.393 , $p = 0.07$). The DISTLM involving BSS and river flows included BSS₃₆₅, Flow₁₀₀ and
 36 Flow₃₆₅ as independent variables. It explained 53.5 % of the total variance of benthic
 37 macrofauna compositions. Its representation through the first plane of a dbRDA accounted
 38 for 49.9 % of this initial variance and here again showed two main orientations (Figure 7C).
 39 The first one, mainly along the first component of the dbRDA, corresponded to the
 40 positioning of the stations along the depth gradient and was mainly cued by BSS₃₆₅. The
 41 second one, mainly along the second component of the dbRDA, separated the 4 cruises, and
 42 was mainly cued by Flow₁₀₀. The contribution of Flow₃₆₅ was poorly described by the first
 43 plane of the dbRDA. When used as supplementary variables, CJD and AJD correlated

1 significantly ($p < 0.05$) with this second orientation. This correlation was slightly higher for
 2 CJD ($r = 0.992$ versus $r = 0.820$).



3

4 **Figure 7. WGMP:** Multivariate analyses of spatiotemporal changes in benthic macrofauna
 5 compositions recorded between 2016 and 2018. Non-Metric Multidimensional Scaling of
 6 benthic macrofauna compositions data for stations*dates during 2016-2018 cruises (A).
 7 Figures refer to stations and symbols to cruises. Solid lines represent trajectories of stations
 8 over time and dotted lines indicate groups of stations*dates issued from hierarchical
 9 clustering. Distance-based Redundancy Analysis based on surface sediment characteristics
 10 (B). Distance-based Redundancy Analysis based on integrated BSS and river flows (C).
 11 Station depth (*d-St*), Annual Julian Days (*AJD*) and Cumulated Julian Days (*CJD*) were used
 12 as supplementary variables. Chl-*a*: Chlorophyll-*a*; THAA; Total Hydrolysable Amino Acids;
 13 BSS_365: integrated Bottom Shear Stress over 365 days; Flow_100 and Flow_365:
 14 integrated river flows over 100 and 365 days.

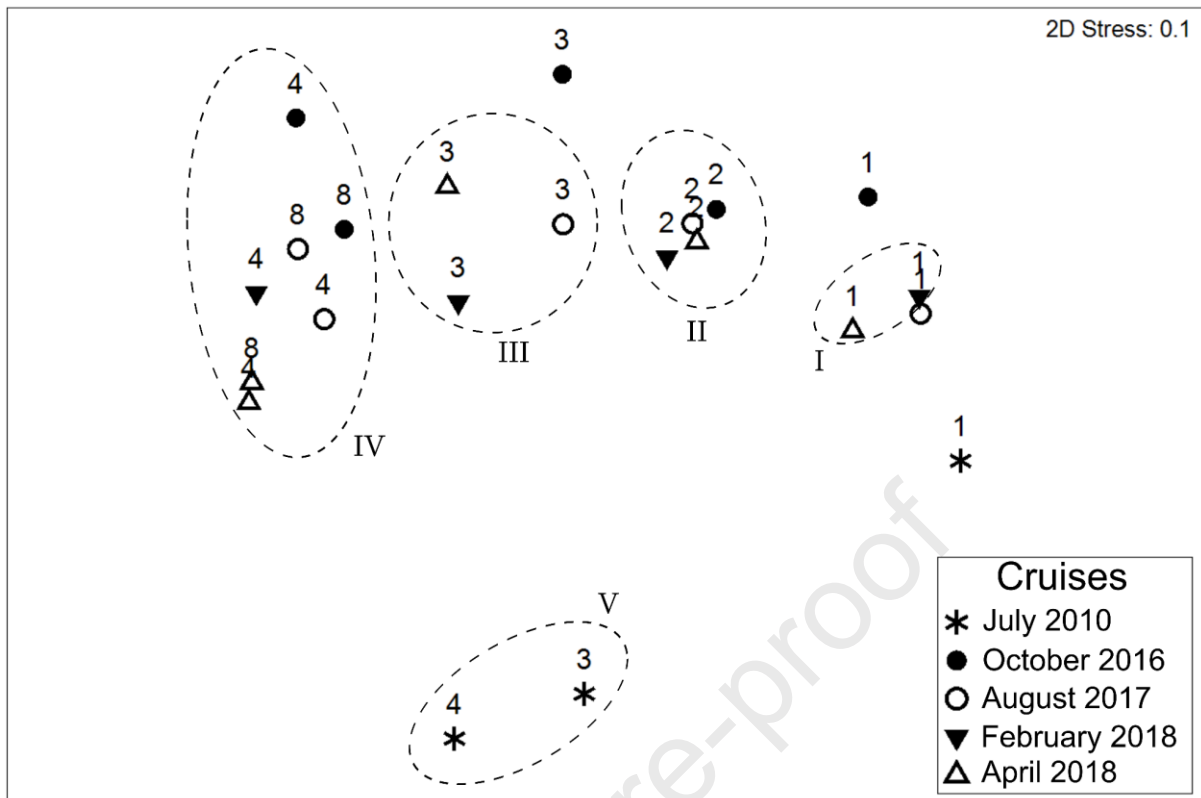
1 **Table II.** *WGMP*: Mean values (\pm standard deviations for replicated measures) of surface sediment and main univariate benthic macrofauna
 2 characteristics during the 4 cruises achieved between 2016 and 2018. $D_{0.5}$: median grain size, SSA: Sediment Surface Area, POC: Particulate
 3 Organic Carbon, Chl-*a*: Chlorophyll-*a*, Phaeo-*a*: Phaeophytin-*a*, THAA: Total Hydrolyzable Amino Acids, EHAA: Enzymatically Hydrolyzable
 4 Amino Acids, SR: Species Richness and J' : Pielou's evenness.

Cruise	Station	$D_{0.5}$ (μm)	SSA ($\text{m}^2\cdot\text{gDW}^{-1}$)	POC ($\text{mg}\cdot\text{m}^{-2}$ SSA)	Chl- <i>a</i> ($\mu\text{g}\cdot\text{gDW}^{-1}$)	Phaeo- <i>a</i> ($\mu\text{g}\cdot\text{gDW}^{-1}$)	Chl- <i>a</i> /(Chl- <i>a</i> +Phaeo- <i>a</i>) (%)	THAA ($\text{mg}\cdot\text{gDW}^{-1}$)	EHAA ($\text{mg}\cdot\text{gDW}^{-1}$)	EHAA/THAA (%)	$\delta^{13}\text{C}$ (‰)	Abundance ($\text{ind}\cdot\text{m}^{-2}$)	Biomass ($\text{mgAFDW}\cdot\text{m}^{-2}$)	SR ($\text{taxa}\cdot 0.75\text{m}^{-2}$)	J'
October 2016	1	60.0	5.0	0.97	0.36 \pm 0.10	2.95 \pm 0.27	10.9 \pm 2.0	0.69 \pm 0.06	0.18 \pm 0.05	26.5 \pm 4.5	-18.11 \pm 0.41	544.0 \pm 198.9	1969.2 \pm 2260.5	38	0.73
	2	26.0	6.1	1.14	0.90 \pm 0.36	8.27 \pm 1.05	10.0 \pm 4.6	2.13 \pm 0.13	0.44 \pm 0.06	20.7 \pm 1.8	-23.20 \pm 0.05	410.7 \pm 112.0	4473.4 \pm 4494.1	30	0.69
	3	20.0	8.1	1.42	0.94 \pm 0.02	8.39 \pm 1.11	10.2 \pm 1.3	2.77 \pm 0.10	0.45 \pm 0.02	16.4 \pm 1.1	-23.23 \pm 0.13	141.3 \pm 68.2	474.2 \pm 433.1	16	0.89
	8	23.1	7.5	1.43	0.87 \pm 0.35	6.75 \pm 0.37	11.3 \pm 4.2	3.60 \pm 0.23	0.53 \pm 0.07	14.9 \pm 2.6	-23.16 \pm 0.08	228.0 \pm 28.0	1922.4 \pm 890.6	27	0.88
	4	20.1	10.3	1.49	1.39 \pm 0.47	9.59 \pm 1.69	13.0 \pm 5.8	4.49 \pm 0.27	0.65 \pm 0.12	14.6 \pm 3.2	-23.01 \pm 0.03	92.0 \pm 42.3	796.2 \pm 418.2	18	0.92
August 2017	1	75.8	2.5	1.15	0.23 \pm 0.09	1.46 \pm 0.46	13.4 \pm 2.5	0.51 \pm 0.18	0.16 \pm 0.04	32.2 \pm 3.8	-24.44 \pm 0.35	784.0 \pm 360.6	958.1 \pm 552.5	43	0.67
	2	23.8	7.3	1.27	1.15 \pm 0.20	6.65 \pm 0.88	14.9 \pm 2.7	3.23 \pm 0.29	0.61 \pm 0.02	18.9 \pm 1.4	-24.22 \pm 0.55	294.7 \pm 109.3	1405.8 \pm 259.1	26	0.68
	3	21.2	8.4	1.28	0.87 \pm 0.05	6.07 \pm 1.64	13.1 \pm 3.2	3.97 \pm 0.07	0.66 \pm 0.10	16.5 \pm 2.2	-24.46 \pm 0.10	218.7 \pm 154.6	754.9 \pm 189.9	24	0.67
	8	24.4	7.6	1.40	0.77 \pm 0.29	5.25 \pm 0.57	12.7 \pm 4.0	3.55 \pm 0.10	0.44 \pm 0.01	12.3 \pm 0.5	-24.22 \pm 0.19	89.3 \pm 43.1	1081.0 \pm 1147.4	18	0.92
	4	21.9	9.3	1.50	0.91 \pm 0.18	6.90 \pm 1.28	12.0 \pm 4.0	4.10 \pm 0.19	0.38 \pm 0.02	9.1 \pm 0.5	-24.03 \pm 0.38	176.0 \pm 60.4	2569.4 \pm 1698.6	27	0.92
February 2018	1	92.0	1.9	0.89	0.52 \pm 0.37	2.53 \pm 1.58	16.4 \pm 1.8	0.72 \pm 0.32	0.29 \pm 0.12	41.0 \pm 2.0	-25.12 \pm 0.23	840.0 \pm 342.0	1625.4 \pm 541.0	32	0.62
	2	17.5	14.2	1.16	2.09 \pm 0.72	9.61 \pm 2.47	17.6 \pm 1.5	3.10 \pm 0.16	0.59 \pm 0.14	19.0 \pm 4.2	-24.58 \pm 0.48	269.3 \pm 217.0	1149.6 \pm 1093.7	35	0.81
	3	23.7	6.2	1.58	0.96 \pm 0.19	6.22 \pm 0.63	13.3 \pm 1.3	2.87 \pm 0.43	0.45 \pm 0.06	15.7 \pm 0.3	-24.41 \pm 0.01	174.7 \pm 130.1	1113.3 \pm 1190.6	27	0.85
	4	17.4	12.6	1.32	1.12 \pm 0.17	9.51 \pm 1.86	10.6 \pm 1.0	4.32 \pm 0.43	0.57 \pm 0.07	13.3 \pm 3.0	-23.91 \pm 0.10	162.7 \pm 112.4	1313.4 \pm 1035.7	22	0.88
April 2018	1	16.3	12.9	0.93	0.66 \pm 0.05	3.67 \pm 0.38	15.2 \pm 0.5	0.98 \pm 0.51	0.26 \pm 0.04	29.6 \pm 11.0	-24.29 \pm 0.002	821.3 \pm 615.5	1271.2 \pm 175.0	35	0.62
	2	15.8	11.0	1.44	4.54 \pm 1.96	18.16 \pm 8.17	20.1 \pm 0.6	3.94 \pm 0.67	0.56 \pm 0.07	14.2 \pm 1.4	-24.05 \pm 0.05	314.7 \pm 32.6	1569.5 \pm 1071.7	25	0.67
	3	17.9	7.7	1.49	3.48 \pm 1.98	15.57 \pm 8.18	18.1 \pm 0.6	4.65 \pm 1.44	0.56 \pm 0.11	12.2 \pm 1.2	-24.11 \pm 0.20	134.7 \pm 50.0	306.8 \pm 354.9	25	0.84
	8	16.2	10.0	1.48	3.99 \pm 1.66	18.37 \pm 6.26	17.6 \pm 2.1	4.36 \pm 0.26	0.61 \pm 0.03	14.0 \pm 0.9	-23.69 \pm 0.18	388.0 \pm 69.4	1522.5 \pm 1301.5	28	0.62
	4	17.4	8.9	1.79	5.86 \pm 0.85	29.35 \pm 2.83	16.6 \pm 1.3	4.65 \pm 0.49	0.72 \pm 0.20	15.3 \pm 2.8	-23.74 \pm 0.31	882.7 \pm 202.6	4985.9 \pm 5475.4	33	0.45

3.4. WGMP: Long-term spatiotemporal changes (2010/2016-2018) in benthic macrofauna compositions

The long-term comparison of univariate benthic macrofauna descriptors highlighted major differences between the July 2010 cruise (Massé et al., 2016) and the 4 cruises of the 2016-2018 period. Species richness values were in the same order of magnitude in July 2010 (32, 22 and 21 taxa at stations 1, 3 and 4, respectively) and in 2016-2018 (means of 37, 23 and 25 taxa at stations 1, 3 and 4, respectively). Conversely, abundances were much higher at station 1 in July 2010 than during all 2016-2018 cruises (1628.0 vs 747.3 ± 137.5 ind.m⁻², respectively). Abundances were also higher at station 3 in July 2010 (328.0 vs 167.4 ± 38.5 ind.m⁻²). They conversely tended to be equivalent at station 4 (118.7 in July 2010 vs 155.0 ± 43.4 ind.m⁻² during 2016-2018 cruises) when excluding the rarely present individuals identified in April 2018 (see section 3.3). Biomasses were higher at stations 1 and 3 in July 2010 (4696.0 and 3495.7 mgAFDW.m⁻², respectively) than during the 2016-2018 cruises (means of 1456.0 ± 437.5 and 662.3 ± 353.0 mgAFDW.m⁻², respectively). They also tended to be equivalent at station 4 between July 2010 (1901.9 mgAFDW.m⁻²) and 2016-2018 cruises (1374.2 ± 436.1 mgAFDW.m⁻²) when excluding the large and rarely present individuals identified at station 4 during August 2017 and April 2018 (see above).

The representation of stations*dates through the nMDS based on macrofauna abundance data from the 2010 and 2016-2018 cruises is shown in Figure 8. The horizontal dimension accounted for the positioning of stations along the depth gradient, whereas the vertical dimension separated sampling dates and more specifically July 2010 (Massé et al., 2016) from all the 2016-2018 cruises. Hierarchical clustering confirmed this pattern with the identification of 5 clusters. The first 4 were almost identical to those of the analysis conducted on the sole 2016-2018 data (see above) and group V was only constituted by stations 3 and 4 in July 2010. The positioning of stations*dates along the horizontal dimension were similar in 2010 and 2016-2018 as opposed to their positioning along the second dimension, which showed important differences in benthic macrofauna compositions between the 2010 and 2016-2018 cruises and suggested that these differences were larger at stations 3 and 4 than at station 1. Average dissimilarity between station 1*July 2010 and stations 1 from 2016-2018 cruises was 43.6 % with *Kurtiella* (14.7 %), *Owenia* (4.7 %), *Gammarus* (4.1 %) and *Ampelisca* (4.0 %) genus contributing most. All these genus were more abundant in July 2010 than in 2016-2018. Average dissimilarity between station 3*July 2010 and stations 3 from 2016-2018 cruises was 67.3 % with *Gammarus* (12.6 %), *Scalibregma* (12.3 %), *Nepthys* (6.0 %) and *Terebellides* (6.0 %) genus contributing most and being more abundant in July 2010 as well. Average dissimilarity between station 4*July 2010 and stations 4 from 2016-2018 cruises was 69.6 % with *Gammarus* (10.0 %), *Ampelisca* (8.6 %), *Hyala* (7.2 %) and *Lumbrineris* (5.3 %) genus contributing most. *Gammarus* and *Lumbrineris* genus were absent during 2016-2018, whereas *Hyala* and *Ampelisca* were less abundant in 2010.



1 **Figure 8:** WGMP: non-Metric Multidimensional Scaling of long-term (i.e., 2010-2018)
 2 spatiotemporal changes in benthic macrofauna compositions. Data for stations*
 3 dates have been collected during both the 2010 and 2016-2018 cruises. Figures refer to stations and
 4 symbols to cruises. Dotted lines indicate the groups of samples issued from hierarchical
 5 clustering.

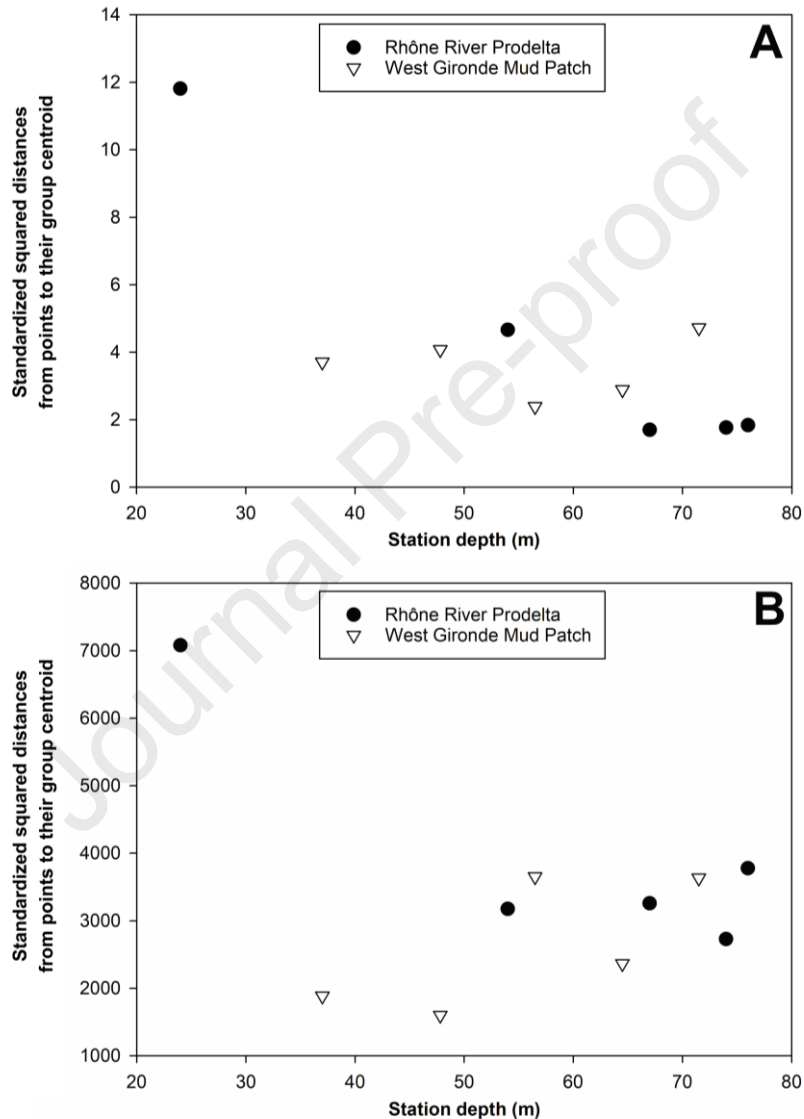
6

7 3.5. Comparison of short-term spatiotemporal changes in surface sediment 8 characteristics and benthic macrofauna compositions within the WGMP and the RRP

9

10 The relationships between station depth and short-term intra-station temporal
 11 variabilities in surface sediment characteristics and benthic macrofauna compositions both
 12 largely differed in the WGMP and the RRP (Figure 9). In both cases and although caution
 13 should clearly be taken when comparing absolute values of WGMP and RRP data, the
 14 highest intra-station variabilities were associated with the RRP shallowest station. Short-term
 15 intra-station temporal variabilities in RRP surface sediment characteristics decreased with
 16 station depth. They mostly resulted from important temporal changes in EHAA, $D_{0.5}$,
 17 EHAA/THAA and Chl-*a* at the shallowest station (i.e., station A). At the 3 deepest stations,
 18 short-term temporal variabilities were low and mostly resulted from limited changes in
 19 EHAA/THAA and Phaeo-*a*. Conversely, short-term intra-station temporal variabilities in
 20 surface sediment characteristics in the WGMP did not show any clear pattern relative to
 21 station depth. These variabilities resulted mostly from changes in $D_{0.5}$ and POC at the
 22 shallowest station (i.e., station 1) *versus* Chl-*a*, Phaeo-*a* and the Chl-*a*/(Chl-*a*+Phaeo-*a*) at all
 23 other stations. Short-term temporal variabilities in benthic macrofauna compositions was
 24 much higher at the shallowest station (i.e., station A) than at the 4 other stations. The
 25 polychaete *Sternaspis scutata* largely contributed to this variability at all stations with higher

1 abundances during July 2011. In the WGMP, short-term intra-station temporal variabilities
 2 were lower at the two shallowest stations, mainly resulting from limited changes in the
 3 abundances of *Amphiura filiformis* (echinoderm), *Kurtiella bidentata* (molluscan) and *Abra*
 4 *alba* (molluscan). They were higher at the 3 deepest stations. At station 3, this mainly
 5 resulted from changes in the abundances of *Amphiura filiformis* (echinoderm), *Ancistrosyllis*
 6 *groenlandica* (polychaete) and *Varicorbula gibba* (molluscan). At stations 8 and 4, this
 7 mainly resulted from high abundances of *Ampelisca spp.* (crustacea) and *Hyala vitrea*
 8 (molluscan) during April 2018.



9

10 **Figure 9.** Comparison between the WGMP and the RRP: Relationship between station depth
 11 and intra-station short-term temporal variabilities (standardized squared distances from points
 12 to their group centroid) in sediment surface characteristics (A) and benthic macrofauna
 13 compositions (B) in both the WGMP (data collected between 2016 and 2018) and the RRP
 14 (data collected between 2007 and 2011; Bonifácio et al. 2014). (See text for details)

15

4. DISCUSSION

4.1. WGMP short-term (2016-2018) spatiotemporal changes

4.1.1. Surface sediment characteristics

Based on the assessments of: (1) the frequency of occurrence of erosional surfaces within the sediment column (Lesueur et al., 1991, 1996; Lesueur and Tastet, 1994) and (2) bioturbation intensities (Jouanneau et al., 1989; Lesueur and Tastet, 1994), early sedimentological surveys concluded that spatial changes within the WGMP mostly take place along the depth gradient with a subdivision between a proximal and a distal part (Lesueur et al., 2002; Lesueur and Tastet, 1994). Relexans et al. (1992) and Massé et al. (2016) achieved preliminary assessments of changes in surface sediment characteristics based on the sampling of a limited number of stations (i.e., 3) along this gradient. Their studies were recently deepened by the use of sediment profile imaging and the assessments of a comprehensive qualitative and quantitative set of surface sedimentary organics characteristics at a much larger number (i.e., 32) of stations sampled during the same cruise (Lamarque et al., 2021). Results supported the correlation between station depths and spatial changes in WGMP surface sediment characteristics.

Our own results clearly show the higher importance of spatial relative to short-term temporal changes in surface sediment characteristics. Station 1 was the only station located in the proximal part. It presented coarser surface sediments during 3 cruises (i.e., October 2016, August 2017 and February 2018) than during April 2018. Such temporal changes may result from the transient deposition of coarse sediments during high-energy events (Lesueur et al., 2002, 2001). It should, however, be pointed out that a strong spatial heterogeneity in surface sediment granulometry at 7 simultaneously sampled stations located within the WGMP proximal part has also been reported (Lamarque et al. 2021), which highlights the difficulty in unambiguously unravelling spatial and temporal changes. Along the same line, the surface sediment collected at station 1 in April 2018 tended to be slightly coarser than the deep old underlying mud (B. Lamarque and N. Dubosq, personal observations), which may be indicative of the transient sedimentation of fine particles as well. All other sampled stations were located in the distal part. They showed significantly different surface sediment characteristics as compared to station 1. They presented restricted spatial changes in surface sediment granulometry, but conversely a clear increase in organic contents (i.e., POC and THAA) as well as a clear decrease in EHAA/THAA with station depth. Moreover, $\delta^{13}\text{C}$ did not show any clear spatial pattern. These results support previous conclusions based on a snapshot synoptic sampling (Lamarque et al. 2021), namely: (1) the subdivision of the WGMP in a proximal and a distal part, (2) the existence of depth gradients for both qualitative and quantitative characteristics of surface sedimentary organics within the distal part, and (3) the mixing of continental and marine sources of particulate organic matter before its sedimentation in the WGMP. The results of the DISTLM/dbRDA analysis achieved in the present study further support the predominant role of local hydrodynamics as the driving factor of the spatial structuration of surface sediment characteristics in the WGMP.

1 They also suggest a lack of significant impact of the Gironde Estuary flow. Caution should
2 nevertheless clearly be taken in interpreting these results due to: (1) co-correlations between
3 station depth, BSS and surface sediment characteristics, and (2) the clear limitations of the
4 use of river flows (which do not include a spatial component during each individual cruise) as
5 a proxy of (particle) riverine inputs to the WGMP.
6

7 At all stations, surface sediments showed higher chloro-pigment concentrations and Chl-
8 *a*/(Chl-*a*+Phaeo-*a*) in April 2018 than during the 3 other cruises. A similar seasonal pattern
9 has already been reported by Relexans et al. (1992) for two stations sampled in the distal part
10 of the WGMP. The seasonality of primary production in this area of the Bay of Biscay is
11 characterized by the occurrence of a spring phytoplankton bloom (Herbland et al., 1998;
12 Labry et al., 2002). Both fluorescence profiles and satellite image analyses (Copernicus
13 Sentinel data 2018, processed by ESA; Chl-*a* computed using SNAP software, data available
14 on request to B. Lamarque) confirmed that the period immediately preceding the April 2018
15 cruise was characterized by high values (i.e., ca. 10 mg.m⁻³) off the mouth of the Gironde
16 Estuary. Our interpretation is thus that the high chloro-pigment concentrations recorded in
17 April 2018 likely resulted from the sedimentation of this bloom. The importance of the
18 seasonal component in driving short-term temporal changes in surface sediment
19 characteristics is further supported by the results of the DISTLM/dbRDA analysis, showing
20 that temporal changes correlate better with Flow₁₀₀ and to a lesser extent BSS₁₀₀ than with
21 Flow₃₆₅ and BSS₃₆₅. This seasonal component dominated short-term temporal changes at the
22 4 stations located in the distal part but not at station 1, where short-term temporal changes in
23 surface sediment characteristics largely result from transient sedimentation following
24 hydrodynamic events (Lesueur et al. 2001, see also above).
25

26 **4.1.2. Benthic macrofauna**

27

28 Before the present study, the only WGMP benthic macrofauna quantitative data had
29 been collected at 3 stations sampled during a single cruise (Massé et al. 2016). Our results
30 thus constitute the first comprehensive data set allowing for a sound assessment of short-term
31 spatiotemporal changes in benthic macrofauna compositions in the area. As for surface
32 sediment characteristics (see above), they clearly show the higher importance of spatial
33 relative to short-term temporal changes.
34

35 All stations presented significantly different macrofauna compositions, except for
36 stations 8 and 4 (Figure 7). As evidenced by their representations in the nMDS first plan,
37 benthic macrofauna compositions changed gradually in relation with station depth. This
38 supports and complements the pattern observed in July 2010 by Massé et al. (2016), which
39 was strongly dominated by differences between the proximal (i.e., station 1) and the distal
40 (i.e., stations 3 and 4) parts. During the present study, stations 1 and 2 were dominated by
41 *Amphiura filiformis* and *Kurtiella bidentata*, which is consistent with the presence of the *A.*
42 *filiformis*-*K. bidentata*-*Abra nitida* community in cohesive muddy sands off wave exposed
43 coast (Hiscock, 1984; Picton et al., 1994). This corresponds to the A5.351 (“*Amphiura*
44 *filiformis*, *Kurtiella bidentata* and *Abra nitida* in circalittoral sandy mud”) habitat of the

1 EUNIS classification (Bajjouk et al., 2015). Deeper stations were all strongly bioturbated
2 (Lamarque et al. 2021 and unpubl. data) and characterized by the presence of: (1) a large
3 variety of polychaetes, (2) seapens (*Cavernularia pusilla* and *Veretillum cynomorium*) and
4 (3) *Nephrops norvegicus* (G. Bernard, personal observation based on sediment trawling).
5 They therefore can be related with the EUNIS A5.361 (“Seapens and burrowing megafauna
6 in circalittoral fine mud”) habitat (Bajjouk et al., 2015).
7

8 Benthic macrofauna abundances presented a strong decreasing trend along the depth
9 gradient (if omitting the exceptional presence of numerous individuals of *Ampelisca spp.* and
10 *Hyala vitrea* at stations 8 and 4 in April 2018), which is conform to the trend already
11 observed by Massé et al. (2016). Such a decreasing pattern is not fully consistent with the
12 results of surveys achieved in other RiOMar, where increasing trends in benthic macrofauna
13 abundances with the distance to the river mouth have been most often observed
14 (Akoumianaki et al., 2013; Aller and Aller, 1986; Alongi et al., 1992; Bonifácio et al., 2014;
15 Rhoads et al., 1985) and interpreted as being conform to the Rhoads et al. (1985) model,
16 according to which the maturity and the abundance of benthic macrofauna communities at the
17 immediate vicinity of river mouths are limited by the sediment instability induced by riverine
18 inputs. During the present study, we attempted to unravel the effects of riverine inputs and
19 local hydrodynamics (as respectively approached by river flows and BSS integrated over two
20 different periods) on the spatiotemporal structuration of benthic macrofauna through the use
21 of DISTLM/dbRDA. Spatial changes in benthic macrofauna compositions correlated best
22 with BSS₃₆₅ and not significantly with river flows. As for surface sediment characteristics
23 (see the section above), caution should be taken in interpreting these results. Nevertheless,
24 they suggest that estuarine inputs probably do not constitute the main factor controlling
25 sediment instability (and thus benthic macrofauna composition) in the WGMP. This
26 conclusion is further supported by the lack of modern sedimentation in the proximal part and
27 by the frequent presence of vertical erosion sequences within its sediments (Lesueur et al.,
28 2002, 2001; Lesueur and Tastet, 1994). As a consequence, our results support the approaches
29 relying on hydrodynamics proposed by McKee et al. (2004) and then Blair & Aller (2012) for
30 the establishment of a typology of marine RiOMar. Within the frame of these typologies, the
31 WGMP would correspond to a type 2/high energy “bypassed” (*sensu* McKee et al. 2004)
32 system where the impact of local hydrodynamics is dominant relative to the one of riverine
33 inputs. The WGMP presents the additional complexity of being composed of two different
34 parts: the proximal one, which is composed of consolidated relict muds deposited ca. 1000
35 years BP (Lesueur et al., 2002) and the distal part, which is the active depocenter (Dubosq et
36 al., 2021). This discrepancy also corresponds to different surface sediment characteristics
37 (Figure 5, Lamarque et al. 2021) and thus to different habitats for benthic macrofauna, which
38 also contributes to differences in benthic macrofauna compositions although these
39 compositions correlated less with individual sediment characteristics than with integrated
40 BSS.
41

42 Overall, short-term temporal changes in benthic macrofauna compositions tended to
43 be larger at deep stations and smaller at the two shallowest stations. Here again, those
44 changes correlated better with environmental parameters than with surface sediment

1 characteristics, with some evidence that short-term temporal changes in benthic macrofauna
2 compositions included both seasonal and inter-annual components. There are several
3 rationales for the occurrence of seasonal changes in benthic macrofauna compositions. First,
4 in the reduced space of the nMDS, individual station trajectories tended to "close" when they
5 were defined based on AJD, which can be considered as indicative of within year/seasonal
6 variability. Second, temporal changes in benthic macrofauna compositions correlated best
7 with Flow₁₀₀, which reflects the correlation between changes in seasonally integrated river
8 flows and benthic macrofauna compositions. Third, AJD correlated significantly with the
9 second component of the dbRDA, which was indicative of temporal changes in benthic
10 macrofauna compositions. There is some indirect evidence for an inter-annual component to
11 short-term temporal changes in benthic macrofauna compositions as well since: (1) a
12 common inter-annual trend was observed at stations 1, 8 and 4, and (2) the second component
13 of the dbRDA correlated slightly better with CJD (indicative of inter-annual/cumulated
14 changes) than with AJD (indicative of within year/seasonal changes only).

15 16 **4.2. WGMP: Long-term comparison (2010/2016-2018) of benthic macrofauna** 17 **compositions**

18
19 The existence of an inter-annual component to temporal changes in benthic
20 macrofauna compositions became even more obvious when 2016-2018 data were compared
21 to those collected in July 2010 (Massé et al., 2016). At the 3 considered stations, differences
22 in benthic macrofauna compositions between 2010 and 2016-2018 were indeed much larger
23 than differences observed during 2016-2018. At all stations, differences in benthic
24 macrofauna compositions relative to July 2010 were maximal in October 2016 and, for most
25 of them, changes occurring during the 2016-2018 period tended to reduce those differences,
26 which is coherent with an ongoing cicatrization process following a major disturbance
27 (Pearson and Rosenberg, 1978) that would have taken place between July 2010 and October
28 2016.

29
30 Sediment characteristics are commonly considered to control benthic macrofauna
31 compositions (Snelgrove and Butman, 1994; Thrush, 1991). The comparison of those
32 characteristics in July 2010 and the 2016-2018 period is complicated by the limited number
33 of parameters that were commonly assessed by Massé et al. (2016) and during the present
34 study. Based on D_{0.5}, POC, Chl-*a*, Phaeo-*a* and Chl-*a*/(Chl-*a*+Phaeo-*a*), there is nevertheless
35 no evidence of changes in surface sediment characteristics between these two periods (data
36 not shown available on request to B. Lamarque). Hence, changes in surface sediment
37 characteristics were unlikely responsible for the long-term changes observed in the benthic
38 macrofauna compositions. In the WGMP, local hydrodynamics is clearly a key factor
39 structuring the spatial distributions of benthic macrofauna composition and activity
40 (Lamarque et al. 2021, see also above). Disturbances of the sediments during strong
41 hydrodynamic events have already been documented based on the analysis of vertical
42 erosional sequences (following resuspension induced by storms) within sediment columns
43 (Lesueur et al., 2002, 1991; Lesueur and Tastet, 1994). It has been estimated that such
44 disturbances occur every ca. 22 years at 35m depth, and only every ca. 80 years at 64m depth

1 (Lesueur et al., 2002). The analysis of the 2010-2018 BSS time series showed higher values
2 during the 2013-2014 winter when the WGMP experienced higher significant wave heights
3 and a longer total storm duration (i.e., 40 and 300 %, respectively) than the overall means of
4 the 1948-2015 period. Overall, the 2013-2014 winter has been the most energetic during the
5 1948-2015 period along most of the European Atlantic coast (Masselink et al., 2016). Storm-
6 induced physical disturbance during this uncommon winter could have affected both surface
7 sediments and benthic macrofauna over the whole WGMP. The duration of successional
8 recovery of benthic macrofauna increases with the spatial scale of the disturbance (Zajac et
9 al. 1998). Cárcamo et al. (2017) have for example shown that, following a major physical
10 disturbance, benthic macrofauna compositions were still not restored to their initial state 3
11 years after a tsunami. Moreover, the fact that the WGMP consists in an isolated habitat (i.e.,
12 surrounded by sand and well separated from other mud patches), which can be entirely
13 physically disturbed also contributes to extend the duration of the cicatrization period by
14 reducing potential for source populations to supply colonists including both mobile adults and
15 pelagic larvae (Probert, 1984; Zajac et al., 1998). Overall, these elements are consistent with
16 the occurrence of a cicatrization process lasting several years in the WGMP after a major
17 disturbance.

18
19 Based on these rationale, our current interpretation of long-term temporal changes in
20 benthic macrofauna compositions within the WGMP is that: (1) the repetition of major
21 storms during the 2013-2014 winter has induced strong physical disturbances of benthic
22 habitats and consequently strong changes in benthic macrofauna compositions over the whole
23 WGMP, and (2) since then temporal changes in benthic macrofauna compositions consist in
24 an ongoing (pluri-annual) cicatrization process superimposed to a seasonal dynamics
25 (Cárcamo et al., 2017). In this context, the increase in long-term temporal changes in benthic
26 macrofauna compositions with station depth may seem counter-intuitive since the intensity of
27 physical disturbance during strong storms is clearly higher at shallower stations. In “normal”
28 conditions (i.e., not during extreme events), shallower stations are, however, also
29 experiencing tougher hydrodynamical conditions than deeper ones. In addition, the frequency
30 of severe storms impacting the sediment column and thus potentially benthic macrofauna
31 compositions (Dobbs and Vozarik, 1983; Glémarec, 1978; Rees et al., 1977) also decreases
32 with station depth (Lesueur et al., 2002). This may result in faster recovery at shallower
33 stations as postulated by Collie et al. (2000) and later tested by Dernie et al. (2003). One can
34 thus assume that resident benthic macrofauna are less resilient to physical disturbance at
35 deeper than at shallower stations, thereby accounting for the larger observed impact at depth.
36 This hypothesis should now be further explored through an extension of the WGMP
37 observation period.

38 39 **4.3. Comparison between the WGMP and the RRP**

40
41 Differences in the spatial zonation of surface sediment characteristics and biological
42 activity traces in the WGMP and the RRP have already been assessed by Lamarque et al.
43 (2021). As for these two sets of variables, the comparison of our own results with those of
44 Bonifácio et al. (2014) highlights the existence of depth gradients in benthic macrofauna

1 compositions within these two systems. These gradients, however, largely differ when
2 considering univariate indices with decreasing abundances with station depth in the WGMP,
3 and conversely higher values at intermediate station depth in the RRP except during July
4 2011 (see also above). Overall, this suggests that the RRP is more conforming to the Rhoads
5 et al. (1985) model (i.e., disturbance of benthic macrofauna mostly due to riverine inputs)
6 than the WGMP.

7
8 Short-term intra-station temporal variabilities in surface sediment characteristics
9 differed between the two systems with a much higher value at the immediate vicinity of the
10 Rhone River Mouth than in the proximal area of the WGMP. In the shallowest area of the
11 RRP, short-term temporal variability in surface sediment characteristics is mainly resulting
12 from high sedimentation taking place during floods (Bonifácio et al., 2014; Cathalot et al.,
13 2010; Pastor et al., 2018). Mostly during autumn and winter, part of these deposits are
14 resuspended initiating a series of resuspension/depositions which result in the displacement
15 of fine particles offshore (Marion et al., 2010; Ulses et al., 2008). During this transfer,
16 particles are sorted relative to their size and the most labile particulate organic matter
17 components are degraded (Bonifácio et al., 2014), which contributes to reduce the magnitude
18 of short-term temporal changes in surface sediment characteristics in deeper areas.
19 Conversely, the magnitude of intra-station short-term temporal changes in surface sediment
20 characteristics tended to be constant all over the WGMP. In the proximal part, the magnitude
21 of these changes is mostly linked to $D_{0.5}$ and related parameters, whereas in the distal part, it
22 mostly results from elevated chloro-pigment concentrations and ratios in April 2018. As
23 opposed to the RRP, the WGMP is not directly connected to the mouth of the Gironde
24 Estuary. Consequently, dilution effects are affecting the whole WGMP, whereas they clearly
25 increase with the distance to the river mouth (and thus station depth) in the RRP (Bourgeois
26 et al., 2011; Cathalot et al., 2013; Lansard et al., 2009; Tesi et al., 2007). Moreover, due to
27 strong local hydrodynamics, the fine particles originating from the Gironde Estuary do not
28 settle in the proximal part of the WGMP (Lesueur et al., 2001), whereas conversely, high
29 sedimentation rates are taking place at the immediate vicinity of the Rhône River Mouth
30 (Miralles et al., 2005; Zuo et al., 1991). Overall, in the proximal part of the WGMP, this
31 contributes to reduce the magnitude of short-term temporal changes in surface sediment
32 characteristics possibly induced by seasonal changes in the hydrological regime of the
33 Gironde Estuary.

34
35 The magnitude of short-term intra-station temporal variabilities in benthic macrofauna
36 compositions showed opposite spatial patterns in the RRP and the WGMP. In both cases,
37 there were differences between shallower and deeper stations. In the RRP, the magnitude of
38 short-term temporal changes was much higher at the immediate vicinity of the Rhône River
39 due to the shift between high and low sedimentation rates during high- and low-flow periods,
40 respectively (Bonifácio et al. 2014). Here again, this pattern largely conforms to the Rhoads
41 et al. (1985) model, which attributes a major role to sedimentation in controlling benthic
42 macrofauna in RiOMar. Conversely, the magnitude of short-term intra-station temporal
43 changes in benthic macrofauna compositions within the WGMP tended to be lower at the 2
44 shallowest stations than at the 3 deepest ones, which was put in relation with a better

1 tolerance/resilience of benthic macrofauna to wave-induced disturbance in the shallowest part
2 of the WGMP (see above). Here again, this pinpoints to differences in the relative roles of
3 riverine inputs and local hydrodynamics in controlling spatiotemporal changes within the two
4 systems.

5
6 Overall, our results further support the characterization of the RRP as a temperate
7 type 1 (i.e., low-energy system with high sedimentation rates) and of the WGMP as
8 temperate type 2 (i.e., high-energy system) RiOMar, respectively. In this sense, they highlight
9 the different mechanisms involved in the control of surface sediment characteristics and
10 benthic macrofauna compositions in line with current RiOMar typologies derived from meta-
11 analyses mainly achieved on tropical and subtropical systems (Blair and Aller, 2012; McKee
12 et al., 2004).

13 14 5. CONCLUSIONS

15
16 The present assessment of short-term (i.e., 2016-2018) spatiotemporal changes in the
17 WGMP surface sediment characteristics confirms the existence of a spatial structuration
18 relative to station depth. This structuration is mainly cued by local hydrodynamics as
19 previously highlighted (Lamarque et al. 2021). Results also demonstrate the presence of a
20 benthic macrofauna spatial gradient characterized by gradual changes in compositions
21 according to station depth. Here again, the control of this spatial structuration is linked to
22 local hydrodynamics integrated over a 1-year period.

23 Both surface sediment characteristics and benthic macrofauna present short-term (i.e.,
24 seasonal and seasonal + inter-annual, respectively) changes best described by $Flow_{100}$ and to
25 a lesser extent BSS_{100} for surface sediment characteristics. Benthic macrofauna compositions
26 also presented long-term (i.e., pluri-annual) changes superimposed over this short-term
27 dynamics. Moreover, the marked shift observed in benthic macrofauna compositions between
28 2010 and 2016-2018 suggests the occurrence of a major disturbance between these two
29 periods, which is currently attributed to the series of severe winter storms that took place
30 during 2013-2014. This highlights the major role of hydrodynamic events in controlling long-
31 term temporal changes in WGMP benthic macrofauna compositions.

32 The comparison between the WGMP and RRP shows major differences in the control
33 of temporal changes in both surface sediment characteristics and benthic macrofauna
34 compositions within their proximal parts. In the RRP, these changes are cued by changes in
35 sedimentation rates in relation with the Rhône River hydrological regime, whereas in the
36 WGMP they result from hydrodynamically-induced transient particle deposition. Another
37 major difference is that, through extreme events, local hydrodynamics is clearly affecting
38 both sediment characteristics and benthic macrofauna compositions over the whole WGMP.
39 These discrepancies further support current RiOMar typologies.

40
41 **Author Contributions:** Conceptualization, B.L., B.D., and A.G.; Data curation, B.L.;
42 Formal analysis, B.L. and A.G.; Funding acquisition, B.D. and A.G.; Investigation, B.L.,
43 B.D., S.S., G.B., N.D., and A.G.; Methodology, B.L., B.D., S.S., M.D. (Mélanie Diaz), F.G.
44 (Florent Grasso), A.S. and A.G.; Resources, B.L., B.D., S.S., G.B., N.D., M.D. (Mélanie

1 Diaz), N.L., F.G. (Frédéric Garabetian), F.G. (Florent Grasso), A.S., S.R., A.R.-R., M.-A.C.,
 2 D.P. and M.D. (Martin Danilo); Validation, B.L., B.D., and A.G.; Visualization, B.L. and
 3 A.G.; Writing—original draft, B.L. and A.G.; Writing—review and editing, B.L., B.D., S.S.,
 4 G.B., N.D., F.G. (Frédéric Garabetian), F.G. (Florent Grasso), S.R., A.R.-R. and A.G. All
 5 authors have read and agreed to the published version of the manuscript.

6

7 **Acknowledgements**

8 This work is part of the PhD thesis of Bastien Lamarque (Bordeaux University). Bastien
 9 Lamarque was partly supported by a doctoral grant from the French “Ministère de
 10 l’Enseignement Supérieur, de la Recherche et de l’Innovation”. This work was supported by:
 11 (1) the JERICO-NEXT project (European Union’s Horizon 2020 Research and Innovation
 12 program under grant agreement no. 654410), (2) the VOG project (LEFE-CYBER and
 13 EC2CO-PNEC), and (3) the MAGMA project (COTE cluster of Excellence ANR-10-LABX-
 14 45). It also benefited from additional fundings allocated by the Conseil Régional Nouvelle-
 15 Aquitaine and the Office Français de la Biodiversité. Operations at sea were funded by the
 16 French Oceanographic Fleet. The authors wish to thank the crew of the R/V Côtes de la
 17 Manche for their help during field sampling, Christophe Fontanier, Marie Claire Perello,
 18 Pascal Lebleu and Hervé Derriennic for their help during sampling and analyses.

19

20 **References**

- 21 Akaike, H., 1973. Information theory as an extension of the maximum likelihood principle,
 22 in: Csaki, F., Petrov, B.N. (Eds.), Proceedings, 2nd International Symposium on
 23 Information Theory. Budapest, pp. 267–281.
- 24 Akoumianaki, I., Papaspyrou, S., Kormas, K.A., Nicolaidou, A., 2013. Environmental
 25 variation and macrofauna response in a coastal area influenced by land runoff. *Estuar.
 26 Coast. Shelf Sci.* 132, 34–44. <https://doi.org/10.1016/j.ecss.2012.04.009>
- 27 Aller, J.Y., Aller, R.C., 1986. General characteristics of benthic faunas on the Amazon inner
 28 continental shelf with comparison to the shelf off the Changjiang River, East China Sea.
 29 *Cont. Shelf Res.* 6, 291–310. [https://doi.org/10.1016/0278-4343\(86\)90065-8](https://doi.org/10.1016/0278-4343(86)90065-8)
- 30 Aller, J.Y., Stupakoff, I., 1996. The distribution and seasonal characteristics of benthic
 31 communities on the Amazon shelf as indicators of physical processes. *Cont. Shelf Res.*
 32 16, 717–751. [https://doi.org/10.1016/0278-4343\(96\)88778-4](https://doi.org/10.1016/0278-4343(96)88778-4)
- 33 Aller, R.C., 1998. Mobile deltaic and continental shelf muds as suboxic, fluidized bed
 34 reactors. *Mar. Chem.* 61, 143–155. [https://doi.org/10.1016/S0304-4203\(98\)00024-3](https://doi.org/10.1016/S0304-4203(98)00024-3)
- 35 Alongi, D.M., Christoffersen, P., Tirendi, F., Robertson, A.I., 1992. The influence of
 36 freshwater and material export on sedimentary facies and benthic processes within the
 37 Fly Delta and adjacent Gulf of Papua (Papua New Guinea). *Cont. Shelf Res.* 12, 287–
 38 326. [https://doi.org/10.1016/0278-4343\(92\)90033-G](https://doi.org/10.1016/0278-4343(92)90033-G)
- 39 Anderson, M., Gorley, R.N., Clarke, K.R., 2008. PERMANOVA + for PRIMER user
 40 manual.
- 41 Anderson, M.J., 2001. A new method for non-parametric multivariate analysis of variance.

- 1 Austral Ecol. 26, 32–46. <https://doi.org/https://doi.org/10.1111/j.1442-9993.2001.01070.pp.x>
- 2
- 3 Bajjouk, T., Guillaumont, B., Michez, N., Thouin, B., Croguennec, C., Populus, J., Louvel-
4 Glaser, J., Gaudillat, V., Chevalier, C., Tourolle, J., Hamon, D., 2015. Classification
5 EUNIS, Système d'information européen sur la nature: Traduction française des
6 habitats benthiques des Régions Atlantique et Méditerranée. Vol. 2. Habitats subtidaux
7 & complexes d'habitats. <https://doi.org/https://archimer.ifremer.fr/doc/00271/38223/>
- 8 Bischl, B., Lang, M., Bossek, J., Horn, D., Richter, J., Surmann, D., 2017. BBmisc:
9 Miscellaneous Helper Functions for B. Bischl. R Packag. version 1-1-1.
- 10 Blair, N.E., Aller, R.C., 2012. The Fate of Terrestrial Organic Carbon in the Marine
11 Environment. *Ann. Rev. Mar. Sci.* 4, 401–423. <https://doi.org/10.1146/annurev-marine-120709-142717>
- 12
- 13 Bonifácio, P., Bourgeois, S., Labrune, C., Amouroux, J.M., Escoubeyrou, K., Buscail, R.,
14 Romero-Ramirez, A., Lantoine, F., Vétion, G., Bichon, S., Desmalades, M., Rivière, B.,
15 Deflandre, B., Grémare, A., 2014. Spatiotemporal changes in surface sediment
16 characteristics and benthic macrofauna composition off the Rhône River in relation to its
17 hydrological regime. *Estuar. Coast. Shelf Sci.* 151, 196–209.
18 <https://doi.org/10.1016/j.ecss.2014.10.011>
- 19 Bourgeois, S., Pruski, A.M., Sun, M.Y., Buscail, R., Lantoine, F., Kerhervé, P., Vétion, G.,
20 Rivière, B., Charles, F., 2011. Distribution and lability of land-derived organic matter in
21 the surface sediments of the Rhône prodelta and the adjacent shelf (Mediterranean Sea,
22 France): A multi proxy study. *Biogeosciences* 8, 3107–3125. <https://doi.org/10.5194/bg-8-3107-2011>
- 23
- 24 Burdige, D.J., 2005. Burial of terrestrial organic matter in marine sediments: A re-
25 assessment. *Global Biogeochem. Cycles* 19, 1–7.
26 <https://doi.org/10.1029/2004GB002368>
- 27 Cárcamo, P.J., Hernández-Miranda, E., Veas, R., Quiñones, R.A., 2017. Macrofaunal
28 community structure in Bahía Concepción (Chile) before and after the 8.8 Mw Maule
29 mega-earthquake and tsunami. *Mar. Environ. Res.* 130, 233–247.
30 <https://doi.org/10.1016/j.marenvres.2017.07.022>
- 31 Castaing, P., Allen, G., Houdart, M., Moign, Y., 1979. Étude par télédétection de la
32 dispersion en mer des eaux estuariennes issues de la Gironde et du Pertuis de
33 Maumusson. *Oceanol. Acta* 2, 459–468.
34 <https://doi.org/https://archimer.ifremer.fr/doc/00122/23361/>
- 35 Castaing, P., Allen, G.P., 1981. Mechanisms controlling seaward escape of suspended
36 sediment from the Gironde: A macrotidal estuary in France. *Mar. Geol.* 40, 101–118.
37 [https://doi.org/10.1016/0025-3227\(81\)90045-1](https://doi.org/10.1016/0025-3227(81)90045-1)
- 38 Castaing, P., Philipps, I., Weber, O., 1982. Répartition et dispersion des suspensions dans les
39 eaux du plateau continental aquitain. *Oceanol. Acta* 5, 85–96.
40 <https://doi.org/https://archimer.ifremer.fr/doc/00121/23193/>

- 1 Cathalot, C., Rabouille, C., Pastor, L., Deflandre, B., Viollier, E., Buscail, R., Grémare, A.,
2 Treignier, C., Pruski, A., 2010. Temporal variability of carbon recycling in coastal
3 sediments influenced by rivers: Assessing the impact of flood inputs in the Rhône River
4 prodelta. *Biogeosciences* 7, 1187–1205. <https://doi.org/10.5194/bg-7-1187-2010>
- 5 Cathalot, C., Rabouille, C., Tisnérat-Laborde, N., Toussaint, F., Kerhervé, P., Buscail, R.,
6 Loftis, K., Sun, M.Y., Tronczynski, J., Azoury, S., Lansard, B., Treignier, C., Pastor, L.,
7 Tesi, T., 2013. The fate of river organic carbon in coastal areas: A study in the Rhône
8 River delta using multiple isotopic ($\delta^{13}\text{C}$, $\delta^{14}\text{C}$) and organic tracers. *Geochim.*
9 *Cosmochim. Acta* 118, 33–55. <https://doi.org/10.1016/j.gca.2013.05.001>
- 10 Cirac, P., Berne, S., Castaing, P., Weber, O., 2000. Processus de mise en place et d'évolution
11 de la couverture sédimentaire superficielle de la plate-forme nord-aquitaine. *Oceanol.*
12 *Acta* 23, 663–686. [https://doi.org/10.1016/s0399-1784\(00\)00110-9](https://doi.org/10.1016/s0399-1784(00)00110-9)
- 13 Clarke, K.R., 1993. Non-parametric multivariate analyses of changes in community structure.
14 *Aust. J. Ecol.* 18, 117–143. [https://doi.org/https://doi.org/10.1111/j.1442-](https://doi.org/https://doi.org/10.1111/j.1442-9993.1993.tb00438.x)
15 [9993.1993.tb00438.x](https://doi.org/https://doi.org/10.1111/j.1442-9993.1993.tb00438.x)
- 16 Clarke, K.R., Somerfield, P.J., Gorley, R.N., 2008. Testing of null hypotheses in exploratory
17 community analyses: similarity profiles and biota-environment linkage. *J. Exp. Mar.*
18 *Bio. Ecol.* 366, 56–69. <https://doi.org/10.1016/j.jembe.2008.07.009>
- 19 Clarke, K.R., Warwick, R.M., 2001. *Change in Marine Communities: An Approach to*
20 *Statistical Analysis and Interpretation*, 2nd edition. PRIMER-E, Plymouth.
- 21 Collie, J.S., Hall, S.J., Kaiser, M.J., Poiner, I.R., 2000. A quantitative analysis of fishing
22 impacts on shelf-sea benthos. *J. Anim. Ecol.* 69, 785–798.
23 <https://doi.org/https://doi.org/10.1046/j.1365-2656.2000.00434.x>
- 24 Constantin, S., Doxaran, D., Derkacheva, A., Novoa, S., Lavigne, H., 2018. Multi-temporal
25 dynamics of suspended particulate matter in a macro-tidal river Plume (the Gironde) as
26 observed by satellite data. *Estuar. Coast. Shelf Sci.* 202, 172–184.
27 <https://doi.org/10.1016/j.ecss.2018.01.004>
- 28 Coplen, T.B., 2011. Guidelines and recommended terms for expression of stable- isotope-
29 ratio and gas-ratio measurement results. *Rapid Commun. Mass Spectrom* 25, 2538–
30 2560. <https://doi.org/10.1002/rcm.5129>
- 31 Deflandre, B., 2018a. JERICOBENT-3 croise, RV Côtes De La Manche.
32 <https://doi.org/10.17600/18000469>
- 33 Deflandre, B., 2018b. JERICOBENT-4 croise, RV Côtes De La Manche.
34 <https://doi.org/10.17600/18000470>
- 35 Deflandre, B., 2017. JERICOBENT-2 croise, RV Côtes De La Manche.
36 <https://doi.org/10.17600/17011000>
- 37 Deflandre, B., 2016. JERICOBENT-1 croise, RV Côtes De La Manche.
38 <https://doi.org/10.17600/16010400>
- 39 Dernie, K.M., Kaiser, M.J., Warwick, R.M., 2003. Recovery rates of benthic communities

- 1 following physical disturbance. *J. Anim. Ecol.* 72, 1043–1056.
2 <https://doi.org/10.1046/j.1365-2656.2003.00775.x>
- 3 Diaz, M., Grasso, F., Le Hir, P., Sottolichio, A., Caillaud, M., Thouvenin, B., 2020. Modeling
4 Mud and Sand Transfers Between a Macrotidal Estuary and the Continental Shelf:
5 Influence of the Sediment Transport Parameterization. *J. Geophys. Res. Ocean.* 125.
6 <https://doi.org/10.1029/2019JC015643>
- 7 Dobbs, F.C., Vozarik, J.M., 1983. Immediate effects of a storm on coastal infauna. *Mar. Ecol.*
8 *Prog. Ser.* 11, 273–279. [https://doi.org/https://doi.org/10.3354/meps011273](https://doi.org/10.3354/meps011273)
- 9 Doxaran, D., Froidefond, J.M., Castaing, P., Babin, M., 2009. Dynamics of the turbidity
10 maximum zone in a macrotidal estuary (the Gironde, France): Observations from field
11 and MODIS satellite data. *Estuar. Coast. Shelf Sci.* 81, 321–332.
12 <https://doi.org/10.1016/j.ecss.2008.11.013>
- 13 Dubosq, N., Schmidt, S., Walsh, J.P., Grémare, A., Gillet, H., Lebleu, P., Poirier, D., Perello,
14 M.C., Lamarque, B., Deflandre, B., 2021. A first assessment of organic carbon burial in
15 the West Gironde Mud Patch (Bay of Biscay). *Cont. Shelf Res.* 221.
16 <https://doi.org/10.1016/j.csr.2021.104419>
- 17 Etcheber, H., Relexans, J.C., Beliard, M., Weber, O., Buscail, R., Heussner, S., 1999.
18 Distribution and quality of sedimentary organic matter on the Aquitanian margin (Bay of
19 Biscay). *Deep. Res. Part II* 46, 2249–2288. [https://doi.org/10.1016/S0967-](https://doi.org/10.1016/S0967-0645(99)00062-4)
20 [0645\(99\)00062-4](https://doi.org/10.1016/S0967-0645(99)00062-4)
- 21 Gadel, F., Jouanneau, J.M., Weber, O., Serve, L., Comellas, L., 1997. Traceurs organiques
22 dans les dépôts de la vasière Ouest-Gironde (Golfe de Gascogne). *Oceanol. Acta* 20,
23 687–695. <https://doi.org/https://archimer.ifremer.fr/doc/00093/20426/>
- 24 Glémarec, M., 1978. Problèmes d'écologie dynamique et de succession en baie de
25 Concarneau. *Vie Milieu* 1–20.
- 26 Grasso, F., Verney, R., Le Hir, P., Thouvenin, B., Schulz, E., Kervella, Y., Khojasteh Pour
27 Fard, I., Lemoine, J.P., Dumas, F., Garnier, V., 2018. Suspended Sediment Dynamics in
28 the Macrotidal Seine Estuary (France): 1. Numerical Modeling of Turbidity Maximum
29 Dynamics. *J. Geophys. Res. Ocean.* 123, 558–577.
30 <https://doi.org/10.1002/2017JC013185>
- 31 Grémare, A., Gutiérrez, D., Anschutz, P., Amouroux, J.M., Deflandre, B., Vétion, G., 2005.
32 Spatio-temporal changes in totally and enzymatically hydrolyzable amino acids of
33 superficial sediments from three contrasted areas. *Prog. Oceanogr.* 65, 89–111.
34 <https://doi.org/10.1016/j.pocean.2005.02.016>
- 35 Harmelin-Vivien, M.L., Bănar, D., Dierking, J., Hermand, R., Letourneur, Y., Salen-Picard,
36 C., 2009. Linking benthic biodiversity to the functioning of coastal ecosystems subjected
37 to river runoff (NW Mediterranean). *Anim. Biodivers. Conserv.* 32, 135–145.
38 <https://doi.org/https://doi.org/10.32800/abc.2009.32.0135>
- 39 Harrell, F.E., 2021. Hmisc: Harrell Miscellaneous. R Packag. version 4-5-0.
- 40 Hedges, J.I., Keil, R.G., 1995. Sedimentary organic matter preservation: an assessment and

- 1 speculative synthesis. *Mar. Chem.* 49, 81–115. [https://doi.org/10.1016/0304-4203\(95\)00008-F](https://doi.org/10.1016/0304-4203(95)00008-F)
- 2
- 3 Herbland, A., Delmas, D., Laborde, P., Sautour, B., Artigas, F., 1998. Phytoplankton spring
4 bloom of the Gironde plume waters in the Bay of Biscay: Early phosphorus limitation
5 and food-web consequences. *Oceanol. Acta* 21, 279–291. [https://doi.org/10.1016/S0399-1784\(98\)80015-7](https://doi.org/10.1016/S0399-1784(98)80015-7)
- 6
- 7 Hiscock, K., 1984. Rocky shore surveys of the Isles of Scilly. March 27th to April 1st and
8 July 7th to 15th 1983. Peterbrgh. Nat. Conserv. Counc. CSD Rep. 509.
- 9 Jalón-Rojas, I., Sottolichio, A., Hanquiez, V., Fort, A., Schmidt, S., 2018. To what extent
10 multidecadal changes in morphology and fluvial discharge impact tide in a convergent
11 (turbid) tidal river. *J. Geophys. Res. Ocean.* 123, 3241–3258.
12 <https://doi.org/10.1002/2017JC013466>
- 13 Jouanneau, J.M., Weber, O., Latouche, C., Vernet, J.P., Dominik, J., 1989. Erosion, non-
14 deposition and sedimentary processes through a sedimentological and radioisotopic
15 study of surficial deposits from the “Ouest-Gironde vasière” (Bay of Biscay). *Cont.*
16 *Shelf Res.* 9, 325–342. [https://doi.org/10.1016/0278-4343\(89\)90037-X](https://doi.org/10.1016/0278-4343(89)90037-X)
- 17 Labry, C., Herbland, A., Delmas, D., 2002. The role of phosphorus on planktonic production
18 of the Gironde plume waters in the Bay of Biscay. *J. Plankton Res.* 24, 97–117.
19 <https://doi.org/10.1093/plankt/24.2.97>
- 20 Lamarque, B., Deflandre, B., Dalto, A.G., Schmidt, S., Romero-Ramirez, A., Garabetian, F.,
21 Dubosq, N., Diaz, M., Grasso, F., Sottolichio, A., Bernard, G., Gillet, H., Cordier, M.A.,
22 Poirier, D., Lebleu, P., Derriennic, H., Danilo, M., Tenório, M.M.B., Grémare, A., 2021.
23 Spatial distributions of surface sedimentary organics and sediment profile image
24 characteristics in a high-energy temperate marine riomar: The west gironde mud patch.
25 *J. Mar. Sci. Eng.* 9, 242. <https://doi.org/10.3390/jmse9030242>
- 26 Lansard, B., Rabouille, C., Denis, L., Grenz, C., 2009. Benthic remineralization at the land-
27 ocean interface: A case study of the Rhône River (NW Mediterranean Sea). *Estuar.*
28 *Coast. Shelf Sci.* 81, 544–554. <https://doi.org/10.1016/j.ecss.2008.11.025>
- 29 Lazure, P., Dumas, F., 2008. An external-internal mode coupling for a 3D hydrodynamical
30 model for applications at regional scale (MARS). *Adv. Water Resour.* 31, 233–250.
31 <https://doi.org/10.1016/j.advwatres.2007.06.010>
- 32 Lesueur, P., Jouanneau, J.M., Boust, D., Tastet, J.P., Weber, O., 2001. Sedimentation rates
33 and fluxes in the continental shelf mud fields in the Bay of Biscay (France). *Cont. Shelf*
34 *Res.* 21, 1383–1401. [https://doi.org/10.1016/S0278-4343\(01\)00004-8](https://doi.org/10.1016/S0278-4343(01)00004-8)
- 35 Lesueur, P., Tastet, J., Weber, O., Sinko, J., 1991. Modèle faciologique d’un corps
36 sédimentaire pélitique de plate-forme la vasière Ouest-Gironde (France). *Oceanol. Acta*
37 11, 143–153. <https://doi.org/https://archimer.ifremer.fr/doc/00267/37871/>
- 38 Lesueur, P., Tastet, J.P., 1994. Facies, internal structures and sequences of modern Gironde-
39 derived muds on the Aquitaine inner shelf, France. *Mar. Geol.* 120, 267–290.
40 [https://doi.org/10.1016/0025-3227\(94\)90062-0](https://doi.org/10.1016/0025-3227(94)90062-0)

- 1 Lesueur, P., Tastet, J.P., Marambat, L., 1996. Shelf mud fields formation within historical
2 times: Examples from offshore the Gironde estuary, France. *Cont. Shelf Res.* 16, 1849–
3 1870. [https://doi.org/10.1016/0278-4343\(96\)00013-1](https://doi.org/10.1016/0278-4343(96)00013-1)
- 4 Lesueur, P., Tastet, J.P., Weber, O., 2002. Origin and morphosedimentary evolution of fine-
5 grained modern continental shelf deposits: The Gironde mud fields (Bay of Biscay,
6 France). *Sedimentology* 49, 1299–1320. <https://doi.org/10.1046/j.1365-3091.2002.00498.x>
- 7
- 8 Levin, L.A., Boesch, D.F., Covich, A., Dahm, C., Erséus, C., Ewel, K.C., Kneib, R.T.,
9 Moldenke, A., Palmer, M.A., Snelgrove, P., Strayer, D., Weslawski, J.M., 2001. The
10 function of marine critical transition zones and the importance of sediment biodiversity.
11 *Ecosystems* 4, 430–451. <https://doi.org/10.1007/s10021-001-0021-4>
- 12 Longère, P., Dorel, D., 1970. Etude des sédiments meubles de la vasière de la Gironde et des
13 régions avoisinantes. *Rev. des Trav. l'Institut des Pêches Marit.* 34, 233–256.
- 14 Lotze, H.K., Lenihan, H.S., Bourque, B.J., Bradbury, R.H., Cooke, R.G., Kay, M.C.,
15 Kidwell, S.M., Kirby, M.X., Peterson, C.H., Jackson, J.B.C., 2006. Depletion,
16 Degradation, and Recovery Potential of Estuaries and Coastal Seas. *Science.* 312, 1806–
17 1809. <https://doi.org/10.1126/science.1128035>
- 18 Marion, C., Dufois, F., Arnaud, M., Vella, C., 2010. In situ record of sedimentary processes
19 near the Rhône River mouth during winter events (Gulf of Lions, Mediterranean Sea).
20 *Cont. Shelf Res.* 30, 1095–1107. <https://doi.org/10.1016/j.csr.2010.02.015>
- 21 Massé, C., Meisterhans, G., Deflandre, B., Bachelet, G., Bourasseau, L., Bichon, S., Ciutat,
22 A., Jude-Lemeilleur, F., Lavesque, N., Raymond, N., Grémare, A., Garabetian, F., 2016.
23 Bacterial and macrofaunal communities in the sediments of the West Gironde Mud
24 Patch, Bay of Biscay (France). *Estuar. Coast. Shelf Sci.* 179, 189–200.
25 <https://doi.org/10.1016/j.ecss.2016.01.011>
- 26 Masselink, G., Castello, B., Scott, T., Dodet, G., Suanez, S., Jackson, D., Floc'h, F., 2016.
27 Extreme wave activity during 2013/2014 winter and morphological impacts along the
28 Atlantic coast of Europe. *Geophys. Res. Lett.* 43, 2135–2143.
29 <https://doi.org/10.1002/2015GL067492>. Received
- 30 Mayer, L.M., 1994. Surface area control of organic carbon accumulation in continental shelf
31 sediments. *Geochim. Cosmochim. Acta* 58, 1271–1284.
32 [https://doi.org/10.1016/0016-7037\(94\)90381-6](https://doi.org/10.1016/0016-7037(94)90381-6)
- 33 Mayer, L.M., Linda L., S., Sawyer, T., Plante, C.J., Jumars, P.A., Sel, R.L., 1995.
34 Bioavailable amino acids in sediments: A biomimetic, kinetics based approach. *Limnol.*
35 *Oceanogr.* 40, 511–520. <https://doi.org/10.4319/lo.1995.40.3.0511>
- 36 McKee, B.A., Aller, R.C., Allison, M.A., Bianchi, T.S., Kineke, G.C., 2004. Transport and
37 transformation of dissolved and particulate materials on continental margins influenced
38 by major rivers: Benthic boundary layer and seabed processes. *Cont. Shelf Res.* 24, 899–
39 926. <https://doi.org/10.1016/j.csr.2004.02.009>
- 40 Medernach, L., Grémare, A., Amoureux, J.M., Colomines, J.C., Vétion, G., 2001. Temporal

- 1 changes in the amino acid contents of particulate organic matter sedimenting in the Bay
2 of Banyuls-sur-Mer (northwestern Mediterranean). *Mar. Ecol. Prog. Ser.* 214, 55–65.
3 <https://doi.org/10.3354/meps214055>
- 4 Miralles, J., Radakovitch, O., Aloisi, J.C., 2005. 210Pb sedimentation rates from the
5 Northwestern Mediterranean margin. *Mar. Geol.* 216, 155–167.
6 <https://doi.org/10.1016/j.margeo.2005.02.020>
- 7 Neveux, J., Lantoiné, F., 1993. Spectrofluorometric assay of chlorophylls and phaeopigments
8 using the least squares approximation technique. *Deep. Res. Part I* 40, 1747–1765.
9 [https://doi.org/10.1016/0967-0637\(93\)90030-7](https://doi.org/10.1016/0967-0637(93)90030-7)
- 10 Oksanen, J., Blanchet, F.G., Friendly, M., Kindt, R., Legendre, P., McGlinn, D., Minchin,
11 P.R., O’Hara, R.B., Simpson, G.L., Solymos, P., Stevens, M.H.H., Szoecs, E., Wagner,
12 H., 2019. *vegan: Community Ecology Package*. R Packag. version 2-5-6.
- 13 Parra, M., Castaing, P., Jouanneau, J.M., Grousset, F., Latouche, C., 1998. Nd-Sr isotopic
14 composition of present-day sediments from the Gironde Estuary, its draining basins and
15 the WestGironde mud patch (SW France). *Cont. Shelf Res.* 19, 135–150.
16 [https://doi.org/10.1016/S0278-4343\(98\)00083-1](https://doi.org/10.1016/S0278-4343(98)00083-1)
- 17 Pastor, L., Deflandre, B., Viollier, E., Cathalot, C., Metzger, E., Rabouille, C., Escoubeyrou,
18 K., Lloret, E., Pruski, A.M., Vétion, G., Desmalades, M., Buscaïl, R., Grémare, A.,
19 2011. Influence of the organic matter composition on benthic oxygen demand in the
20 Rhône River prodelta (NW Mediterranean Sea). *Cont. Shelf Res.* 31, 1008–1019.
21 <https://doi.org/10.1016/j.csr.2011.03.007>
- 22 Pastor, L., Rabouille, C., Metzger, E., Thibault de Chanvalon, A., Viollier, E., Deflandre, B.,
23 2018. Transient early diagenetic processes in Rhône prodelta sediments revealed in
24 contrasting flood events. *Cont. Shelf Res.* 166, 65–76.
25 <https://doi.org/10.1016/j.csr.2018.07.005>
- 26 Pearson, T.H., Rosenberg, R., 1978. Macrobenthos succession in relation to organic
27 enrichment and pollution of the marine environment. *Oceanogr. Mar. Biol. Annu. Rev.*
28 16, 229–331.
- 29 Picton, B.E., Emblow, C.S., Morrow, C.C., Sides, E.M., Costello, M.J., 1994. Marine
30 communities of the Mulroy Bay and Lough Swill area, north-west Ireland, with an
31 assessment of their nature conservation importance. *Environ. Sci. Unit, Trinity Coll. (f.*
32 *Surv. Report)*.
- 33 Probert, P.K., 1984. Disturbance, sediment stability, and trophic structure of soft-bottom
34 communities. *J. Mar. Res.* 42, 893–921.
35 <https://doi.org/https://doi.org/10.1357/002224084788520837>
- 36 Rees, E.I.S., Nicholaidou, A., Laskaridou, P., 1977. The Effects of Storms on the Dynamics
37 of Shallow Water Benthic Associations. *Biol. Benthic Org.* 465–474.
38 <https://doi.org/10.1016/b978-0-08-021378-1.50052-x>
- 39 Relexans, J.C., Lin, R.G., Castel, J., Etcheber, H., Laborde, P., 1992. Response of biota to
40 sedimentary organic matter quality of the west Gironde mud patch, Bay of Biscay

- 1 (France). *Oceanol. Acta* 15, 639–649.
2 <https://doi.org/https://archimer.ifremer.fr/doc/00101/21231/>
- 3 Rhoads, D.C., Boesch, D.F., Zhican, T., Fengshan, X., Liqiang, H., Nilsen, K.J., 1985.
4 Macrobenthos and sedimentary facies on the Changjiang delta platform and adjacent
5 continental shelf, East China Sea. *Cont. Shelf Res.* 4, 189–213.
6 [https://doi.org/10.1016/0278-4343\(85\)90029-9](https://doi.org/10.1016/0278-4343(85)90029-9)
- 7 Roland, A., Ardhuin, F., 2014. On the developments of spectral wave models: Numerics and
8 parameterizations for the coastal ocean. *Ocean Dyn.* 64, 833–846.
9 <https://doi.org/10.1007/s10236-014-0711-z>
- 10 Snelgrove, P.V.R., Butman, C.A., 1994. Animal Sediment Relationships Revisited – Cause
11 Versus Effect. *Oceanogr. Mar. Biol. an Annu. Rev.* 32, 111–177.
- 12 Soulsby, R., 1997. *Dynamics of Marine Sands: A Manual for Practical Applications*, Thomas
13 Tel. ed.
- 14 Tesi, T., Miserocchi, S., Goñi, M.A., Langone, L., 2007. Source, transport and fate of
15 terrestrial organic carbon on the western Mediterranean Sea, Gulf of Lions, France. *Mar.*
16 *Chem.* 105, 101–117. <https://doi.org/10.1016/j.marchem.2007.01.005>
- 17 Thrush, S.F., 1991. Spatial patterns in soft-bottom communities. *Trends Ecol. Evol.* 6, 75–79.
18 [https://doi.org/https://doi.org/10.1016/0169-5347\(91\)90178-Z](https://doi.org/https://doi.org/10.1016/0169-5347(91)90178-Z)
- 19 Ulses, C., Estournel, C., Durrieu de Madron, X., Palanques, A., 2008. Suspended sediment
20 transport in the Gulf of Lions (NW Mediterranean): Impact of extreme storms and
21 floods. *Cont. Shelf Res.* 28, 2048–2070. <https://doi.org/10.1016/j.csr.2008.01.015>
- 22 Wakeham, S.G., Lee, C., Hedges, J.I., Hernes, P.J., Peterson, M.L., 1997. Molecular
23 indicators of diagenetic status in marine organic matter. *Geochimica Cosmochim. Acta*
24 61, 5363–5369. <https://doi.org/10.5833/jjgs.33.70>
- 25 Weber, O., Jouanneau, J.M., Ruch, P., Mirmand, M., 1991. Grain-size relationship between
26 suspended matter originating in the Gironde estuary and shelf mud-patch deposits. *Mar.*
27 *Geol.* 96, 159–165. [https://doi.org/10.1016/0025-3227\(91\)90213-N](https://doi.org/10.1016/0025-3227(91)90213-N)
- 28 Wheatcroft, R.A., 2006. Time-series measurements of macrobenthos abundance and sediment
29 bioturbation intensity on a flood-dominated shelf. *Prog. Oceanogr.* 71, 88–122.
30 <https://doi.org/10.1016/j.pocean.2006.06.002>
- 31 Worm, B., Barbier, E.B., Beaumont, N., Duffy, J.E., Folke, C., Halpern, B.S., Jackson,
32 J.B.C., Lotze, H.K., Micheli, F., Palumbi, S.R., Sala, E., Selkoe, K.A., Stachowicz, J.J.,
33 Watson, R., 2006. Impacts of biodiversity loss on ocean ecosystem services. *Science*
34 314, 787–790. <https://doi.org/10.1126/science.1132294>
- 35 Zajac, R.N., Whitlatch, R.B., Thrush, S.F., 1998. Recolonization and succession in soft-
36 sediment infaunal communities: The spatial scale of controlling factors. *Hydrobiologia*
37 375–376, 227–240. <https://doi.org/https://doi.org/10.1023/A:1017032200173>
- 38 Zuo, Z., Eisma, D., Berger, G.W., 1991. Determination of sediment accumulation and mixing
39 rates in the Gulf of Lions, Mediterranean Sea. *Oceanol. Acta* 14, 253–262.

1 <https://doi.org/https://archimer.ifremer.fr/doc/00101/21255/>

Journal Pre-proof

Highlights :

- Hydrodynamics leads benthic macrofauna composition in the West Gironde Mud Patch
- Strong storms could also affect benthic macrofauna temporal dynamics in this area
- The West Gironde Mud Patch can be characterized as a temperate high-energy system
- River-dominated Ocean Margins typologies are validated based on macrofauna analysis

Journal Pre-proof

Declaration of interests

The authors declare that they have no known competing financial interests or personal relationships that could have appeared to influence the work reported in this paper.

The authors declare the following financial interests/personal relationships which may be considered as potential competing interests:

Journal Pre-proof